

UCSF

UC San Francisco Electronic Theses and Dissertations

Title

Targeting of an integral membrane protein to the regulated secretory pathway

Permalink

<https://escholarship.org/uc/item/3k18m349>

Author

Waites, Clarissa,

Publication Date

2001

Peer reviewed|Thesis/dissertation

Targeting of an Integral Membrane Protein to the Regulated

Secretory Pathway

by

Clarissa L. Waites

DISSERTATION

Submitted in partial satisfaction of the requirements for the degree of

DOCTOR OF PHILOSOPHY

in

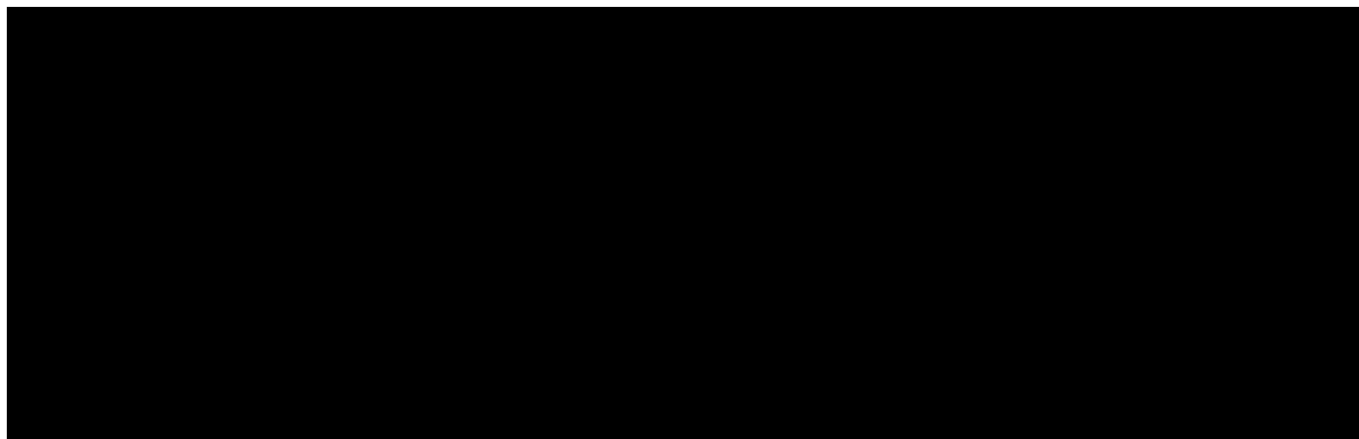
Neuroscience

in the

GRADUATE DIVISION

of the

UNIVERSITY OF CALIFORNIA SAN FRANCISCO



Date

University Librarian

Degree Conferred:

copyright (2001)

by

Clarissa L. Waites

**this thesis is dedicated to my grandmothers, Grammy and Grandma Nona,
who weren't allowed the opportunities that I have taken for granted**

Acknowledgements

I would like to thank the people who have supported me throughout graduate school.

Members of the Edwards laboratory have been indispensable in their friendship, encouragement, guidance, and scientific expertise. I have been extremely fortunate to have such wonderful colleagues. In particular, I would like to thank four post-docs who have been outstanding mentors and teachers during my graduate career: Yongjian Liu, Phil Tan, Dave Krantz, and Rich Reimer. I also owe special thanks to Robert Edwards, who has been an excellent advisor, and whose enthusiasm for science is contagious.

Outside of the lab, I would like to thank my friends from both my undergraduate years at Stanford and from graduate school at UCSF, my parents, and my sister for their constant support and for preserving my sense of humor through this process. Finally, I would like to thank my husband Mark for improving my graduate career, and my life, in every way.

The Rockefeller
University Press

1114 First Avenue, 4th Floor
New York, New York 10021
(212) 327-7938
Fax (212) 327-8587

March 28, 2001

Dr. Clarissa L. Waites

Dear Dr. Waites:

We will grant you permission for the reproduction of JCB-vol:152,1159-1168,2001-article as referred to in your letter dated March 26, 2001.

Permission is granted for one time use only. Please write to us each time for permission concerning future editions and translations, as we do not grant blanket permissions.

Since you are the authors, a credit line is our only requirement.

Please give suitable acknowledgment to the source in the following manner: **Reproduced from *The Journal of Cell Biology*, year, vol., pp.** by copyright permission of The Rockefeller University Press.

Sincerely yours,

THE JOURNAL OF
CELL BIOLOGY

Laura L. Smith
Permissions Coordinator

Laura L. Smith
The Journal of Cell Biology
Permissions
The Rockefeller University Press
1114 First Avenue
New York, NY 10021-8325

Dear Ms. Smith,

I would like to request permission to include in my thesis dissertation a copy of the paper cited below:

Waites, C.L., A. Mehta, P. Tan, E. Friesen, G. Thomas, R. H. Edwards, and D.E. Krantz (2001) An Acidic Motif Retains Vesicular Monoamine Transporter 2 on Large Dense Core Vesicles. *J. Cell Biol.* 152: 1159-1168.

The dissertation will be microfilmed by Bell & Howell (UMI), and they request permission to supply single copies upon demand. Additional copies of the thesis will be disseminated to my thesis committee members and to both the main and Neuroscience Program libraries at the University of California, San Francisco.

Please respond either by email to waites@itsa.ucsf.edu or by fax to (415) 502-5687. Thanks for your consideration.

Sincerely,



Clarissa L. Waites

Advisor Statement

The work presented in Chapter 2 has been published as Waites, CL, Mehta, A, Tan, P, Thomas, G, Edwards, RH, and Krantz, D (2001) An acidic cluster retains vesicular monoamine transporter 2 on large dense core vesicles. *J Cell Biol* 152: 1159-1168. Experiments were performed by Clarissa Waites, with the exception of the *in vitro* phosphorylation of VMAT2 and furin, which was performed by David Krantz. Text was written by Clarissa Waites and Robert Edwards.

The work presented in Chapter 3 is a manuscript in preparation, with the exception of figures 1 and 2. Modified forms of these figures have been published in the paper Krantz, DE, Waites, C, Oorschot, V, Liu, Y, Wilson, R, Tan, P, Klumperman, J, and Edwards, RH (2000) A phosphorylation site regulates sorting of the vesicular acetylcholine transporter to dense core vesicles. *J Cell Biol* 149: 379-395. The experiments in Chapter 3 were performed by Clarissa, and the text was written by her.

Permission to include this work in the thesis was obtained from the Journal of Cell Biology. This work meets the standards required for completion of a PhD in the Neuroscience program at UCSF.



Robert H. Edwards, MD

Thesis advisor

Targeting of an Integral Membrane Protein to the Regulated Secretory

Pathway

Clarissa L. Waites

Abstract

Large dense core vesicles (LDCVs) are one of the major types of secretory vesicle in the brain and play an important role in modulating synaptic transmission. The neuromodulatory properties of LDCVs are derived both from their soluble contents, which are released during exocytosis, and from their integral membrane proteins.

However, little is known about how membrane proteins are targeted to these vesicles. By studying the vesicular monoamine transporter 2 (VMAT2), an integral membrane protein that localizes almost exclusively to LDCVs in neuroendocrine cells, this thesis has identified two C-terminal cytoplasmic motifs that influence targeting to LDCVs. One motif, DDEESESD, is a cluster of acidic amino acids including two serines constitutively phosphorylated by casein kinase 2. The acidic cluster is required for retention of VMAT2 on LDCVs. If this motif is deleted, VMAT2 is removed from LDCVs during their maturation. Thus, the acidic cluster seems to act as a LDCV retention signal. Phosphorylation appears to inactivate this retention signal, suggesting that regulated dephosphorylation of the cluster is required for VMAT2 localization on LDCVs.

Altering the phosphorylation state of the acidic cluster may allow neurons to regulate the amount of VMAT2 that remains on LDCVs. The second motif involved in LDCV targeting is the dileucine-based motif KEEKMAIL. Previous studies have shown that the dileucine-like IL signal is required for VMAT2 endocytosis. This thesis demonstrates that the IL signal and upstream glutamates target VMAT2 to nascent LDCVs in the trans-Golgi network. Replacement of the IL signal or the two glutamates with alanine results in the mistargeting of VMAT2 to the constitutive secretory pathway and its subsequent delivery to the plasma membrane. Thus, these four residues are required for VMAT2 trafficking to LDCVs. These studies provide the first example of a specific LDCV targeting signal, and of a dileucine-based motif involved in sorting to LDCVs. Since the release of monoamines from LDCVs appears to regulate neuronal activity, and the localization of VMAT2 determines the site and mode of monoamine release, the targeting of VMAT2 to LDCVs contributes to the role of monoamine transmitters in neuromodulation.

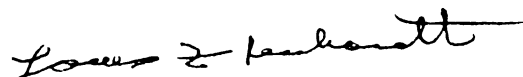


Table of Contents

Dedication	iii
Acknowledgements	iv
Copyright Permission	v
Advisor's Statement	vii
Abstract	viii
List of Figures	xii
CHAPTER ONE: Introduction	1
Synaptic Vesicles and Large Dense Core Vesicles	2
Protein Targeting to SVs and LDCVs	3
Vesicular Neurotransmitter Transporters	4
Vesicular Monoamine Transporter 2 (VMAT2)	5
Acidic Cluster Motifs	7
Dileucine-based Motifs	9
CHAPTER TWO: An Acidic Motif Retains Vesicular Monoamine Transporter 2 on Large Dense Core Vesicles	11
Abstract	12
Introduction	13
Materials and Methods	17
Results	22
Discussion	30
Figures	36

CHAPTER THREE: A Dileucine-like Motif Targets Vesicular Monoamine	
Transporter 2 to the Regulated Secretory Pathway	53
Abstract	54
Introduction	55
Materials and Methods	59
Results	63
Discussion	69
Figures	76
CHAPTER FOUR: Conclusions and Future Directions	88
Conclusions	89
Future Directions	90
References	94

List of Figures

CHAPTER TWO

Figure 1: Analysis of C-terminal VMAT2 deletions by immunofluorescence

Figure 2: Density gradient fractionation of wild type and 507* VMAT2

Figure 3: 507* colocalizes with TGN-38 by immunofluorescence

Figure 4: The 507* deletion localizes to a BFA-resistant compartment that cofractionates with iLDCVs

Figure 5: VMAT2 mutants 507* and DD localize preferentially to immature rather than mature LDCVs

Figure 6: AA and DD VMAT2 differ in the extent of colocalization with SgII

Figure 7: Density gradient fractionation of AA and DD VMAT2

Figure 8: PACS-1 binding to the VMAT2 C-terminus

CHAPTER THREE

Figure 1: Neutralization of glutamates-478 and -479 in VMAT2

Figure 2: The E478A/E479A mutation redistributes VMAT2 away from LDCVs

Figure 3: EE/AA cofractionates with synaptophysin in synaptic-like microvesicles

Figure 4: The I483A/L484A and EE/AA mutations increase delivery of VMAT2 to the plasma membrane

Figure 5: VMAT2 mutants IL/AA and EE/AA enter the constitutive secretory pathway

Figure 6: The IL motif acts prior to the 507* motif in VMAT2 sorting

CHAPTER 1

Introduction

Synaptic Vesicles and Large Dense Core Vesicles

Neurons communicate through the regulated release of signaling molecules from secretory vesicles. There are two primary types of secretory vesicles in the brain, synaptic vesicles (SVs) and large dense core vesicles (LDCVs). Although both undergo regulated exocytosis, they differ in important ways. By electron microscopy, SVs are small, clear vesicles of 30-40 nm diameter that cluster at nerve terminals near the synaptic cleft (Calakos and Scheller, 1996; Kelly, 1993). In contrast, LDCVs are larger (75-125 nm diameter), have an electron-dense core, and appear in dendrites and cell bodies as well as nerve terminals (Kelly, 1993). SVs store classical neurotransmitters including glutamate, γ -aminobutyric acid (GABA) and acetylcholine, as well as monoamine neurotransmitters such as serotonin and dopamine. In contrast, LDCVs store neuromodulatory peptides, growth factors, hormones, and endogenous opioids in addition to monoamines (De Camilli and Jahn, 1990; Martin, 1994). SVs mediate the rapid release of neurotransmitter into the synaptic cleft following an action potential. In contrast, LDCVs release their contents more slowly and in response to different stimuli, consistent with their neuromodulatory role (Kelly, 1993; Martin, 1994).

SVs and LDCVs also differ in their formation. LDCVs bud directly from the trans-Golgi network (TGN), where soluble peptides and membrane proteins sort into LDCVs. LDCVs then undergo a maturation process in which their peptide contents are further aggregated into a compact, dense core, and membrane proteins destined for other

compartments such as lysosomes are removed (Bauerfeind and Huttner, 1993; Kelly and Grote, 1993; Tooze et al., 1993). SVs do not bud from the TGN, but rather form at the nerve terminal near their site of release. Membrane proteins destined for SVs sort into constitutively secreted vesicles in the TGN, are delivered to the cell surface, and enter SVs either directly upon endocytosis or after recycling through endosomes (Bauerfeind and Huttner, 1993; Kelly, 1993; Kelly and Grote, 1993). Since all classical neurotransmitters are synthesized in the cytoplasm, they must be pumped into both SVs and LDCVs before the vesicles can release them by exocytosis.

Protein Targeting to SVs and LDCVs

Little is known about the signals that target integral membrane proteins to SVs or LDCVs. Sorting signals are typically found in cytoplasmic domains of membrane proteins, where they can interact with the cytosolic sorting machinery required for proper targeting. Only one SV protein, vesicle-associated membrane protein 2 (VAMP2) has a well-characterized SV targeting signal, an amphipathic α -helix (Grote et al., 1995). Studies of protein targeting to LDCVs have focused on their soluble peptide contents, which appear to sort into LDCVs as a result of pH and redox-dependent aggregation in the TGN (Chanat and Huttner, 1991; Rindler, 1998). Very few signals that target integral membrane proteins to LDCVs have been identified. The endothelial protein P-selectin, which localizes to LDCVs in neuroendocrine cells after heterologous expression, is

targeted to LDCVs by the tyrosine-based sequence YGVF (Blagoveshchenskaya et al., 1999). However, this sequence is also responsible for the SV targeting of P-selectin. Indeed, many integral membrane proteins sort to both LDCVs and SVs, making it difficult to identify signals specific for either SV or LDCV targeting. Since such targeting signals presumably interact with cytoplasmic machinery necessary for SV and LDCV formation, it has also been difficult to identify cytoplasmic proteins involved in SV and LDCV biogenesis. Studies in our laboratory have identified an integral membrane protein that targets almost exclusively to LDCVs in neuroendocrine cells. We have used this protein, a vesicular neurotransmitter transporter, to identify specific LDCV targeting signals.

Vesicular Neurotransmitter Transporters

Neurotransmitters are synthesized in the cytoplasm and require packaging into SVs and LDCVs for regulated release. The proteins responsible for this packaging are the vesicular neurotransmitter transporters. At least six vesicular transporters have been identified by molecular cloning, including one that transports GABA and glycine (McIntire et al., 1997), two that transport glutamate (Bellocchio et al., 2000), two that transport monoamines (Erickson et al., 1992; Liu et al., 1992), and one that transports acetylcholine (Erickson et al., 1994; Roghani et al., 1994). In contrast to the plasma membrane transporters, which remove neurotransmitter from the synaptic cleft using a

Na⁺ gradient across the plasma membrane, vesicular transporters use a H⁺ electrochemical gradient across the vesicle membrane, generated by a vacuolar H⁺-ATPase, to drive the exchange of luminal protons for cytoplasmic neurotransmitter.

Vesicular Monoamine Transporter 2 (VMAT2)

The two vesicular monoamine transporters (VMATs) were originally cloned by selection in the neurotoxin N-methyl-4-phenylpyridinium (MPP⁺) (Erickson et al., 1992; Liu et al., 1992; Liu et al., 1992a). VMATs protect cells against MPP⁺ toxicity by transporting the toxin into vesicles, where it is sequestered from its primary site of action in mitochondria. These transporters have 12 putative transmembrane domains, cytoplasmic N- and C-terminal domains, and show similarity to a class of bacterial antibiotic resistance proteins. Non-neuronal cells and neurons in the adrenal medulla express VMAT1, while neurons in the brain and sympathetic nervous system as well as histamine-containing cells express the closely-related VMAT2 (Peter et al., 1995; Weihe et al., 1994). Within neurons, VMAT2 resides primarily on LDCVs, but also on tubulovesicular structures in cell bodies and dendrites as well as on SVs at the nerve terminal (Nirenberg et al., 1996; Nirenberg et al., 1997; Nirenberg et al., 1995). This localization is consistent with the observed release of monoamines from cell bodies, dendrites, and nerve terminals in the brain (Cheramy et al., 1981; Geffen et al., 1976; Heeringa and Abercrombie, 1995; Jaffe et al., 1998; Robertson et al., 1991). Since somatodendritic monoamine release has been

proposed to regulate neuronal activity (Aghajanian and Bunney, 1974; Grace and Bunney, 1995), and the localization of VMAT2 influences the site and mode of monoamine release, VMAT2 expression on LDCVs presumably contributes to the role of monoamines in neuromodulation.

To identify the sequences responsible for the LDCV targeting of VMAT2, we expressed the protein in rat pheochromocytoma (PC12) cells. These adrenal-derived neuroendocrine cells contain both LDCVs and synaptic-like microvesicles (SLMVs) (Greene and Tischler, 1976). Further, PC12 cells store monoamines in LDCVs, demonstrating that they have an endogenous monoamine transporter that localizes to LDCVs (Greene and Rein, 1978). Although this endogenous transporter is VMAT1 (Liu et al., 1992; Liu et al., 1992a), heterologously expressed VMAT2 also localizes almost exclusively to LDCVs (Krantz et al., 2000). In addition, PC12 cells adopt a neuronal phenotype when exposed to nerve growth factor and have been extensively characterized by immunofluorescence and gradient fractionation.

Preliminary studies indicated that the signals responsible for targeting VMAT2 to LDCVs are located in its cytoplasmic C-terminus. Therefore, we have focused on this region in our analyses, constructing C-terminal truncations and point mutations, stably expressing these mutants in PC12 cells, and analyzing their localization with a variety of methods. These studies have identified two discrete motifs, an acidic cluster and a dileucine-like motif, which influence the targeting of VMAT2 to LDCVs. Although

these motifs are found in many integral membrane proteins and have certain well-characterized functions, this thesis demonstrates novel roles for each of them.

Acidic Cluster Motifs

Acidic clusters are common trafficking motifs found in a variety of membrane proteins, including the mannose-6-phosphate receptor, the TGN endoprotease furin, and synaptotagmin (Molloy et al., 1999). These motifs typically contain at least six acidic residues, including one or more serines or threonines constitutively phosphorylated by casein kinase 2. Acidic cluster motifs direct diverse protein sorting events including export from the endoplasmic reticulum, apical/basolateral trafficking in polarized cells, and retrieval to the TGN (Molloy et al., 1999). These sorting events appear to require the binding of a novel cytoplasmic adaptor protein, PACS-1 (phosphofurin acidic cluster sorting protein 1) (Molloy et al., 1999). PACS-1 is functionally related to clathrin adaptor proteins, eps-15 and β -arrestin, cytosolic adaptors that connect membrane proteins to the clathrin sorting machinery (Wan et al., 1998). Indeed, PACS-1 appears to facilitate the association of acidic cluster-containing proteins with the clathrin adaptor protein AP-1 (Molloy et al., 1999; Wan et al., 1998). In addition, PACS-1 binds only to phosphorylated acidic cluster motifs (Wan et al., 1998), providing a way to regulate the trafficking of proteins that contain acidic clusters.

Until this thesis, the TGN endoprotease furin has provided the best-characterized example of how acidic clusters mediate protein trafficking. Furin localizes primarily to the TGN, but low levels are also found on immature LDCVs (Dittie et al., 1997). Retrieval of furin from LDCVs to the TGN is mediated by its acidic cluster, including two serines phosphorylated by casein kinase 2 (Dittie et al., 1997; Jones et al., 1995). Replacement of the serines with aspartate to mimic constitutive phosphorylation increases furin retrieval from LDCVs, whereas replacement with alanine to prevent phosphorylation decreases retrieval and increases furin localization to LDCVs (Dittie et al., 1997; Jones et al., 1995). Additional studies have demonstrated that PACS-1 mediates retrieval, and that PACS-1 binds to the phosphorylated acidic cluster of furin but not to the cluster in its unphosphorylated state (Wan et al., 1998). Thus, furin retrieval from LDCVs is mediated by the binding of PACS-1 to the phosphorylated acidic cluster motif.

Chapter 2 of this thesis describes our characterization of the VMAT2 acidic cluster motif DDEESESD, including two serines which are constitutively phosphorylated by casein kinase 2. As with furin, this motif appears to interact with PACS-1 to mediate the removal of VMAT2 from LDCVs in a phosphorylation-dependent way. Replacement of the serines with aspartate promotes the retrieval of VMAT2 from LDCVs, while replacement with alanine promotes VMAT2 localization to LDCVs. However, we find that deletion of the acidic cluster motif also promotes the removal of VMAT2 from

LDCVs. This removal cannot be PACS-1 dependent or even phosphorylation dependent, as the deletion mutant is missing the entire acidic cluster and does not bind PACS-1.

This work suggests that the acidic cluster motif acts not as a signal for removal from LDCVs, as was previously proposed, but as a signal for retention on LDCVs.

Phosphorylation of the cluster presumably inactivates this retention signal and thereby increases PACS-1-mediated retrieval from LDCVs. Since phosphorylation is constitutive, regulated dephosphorylation of the acidic cluster in VMAT2 must be important for retention on LDCVs.

Dileucine-based Motifs

Dileucine-based signals are also common protein sorting motifs. These motifs typically contain either two leucines, a leucine and a second hydrophobic residue such as leucine, isoleucine, methionine, or valine, or two non-leucine hydrophobic residues (Sandoval and Bakke, 1994). Certain proteins also contain acidic residues 4 and 5 positions upstream of the dileucine signal which can influence its effects (Pond et al., 1995). Dileucine-based motifs mediate a number of protein sorting events, including endocytosis, lysosomal and endosomal targeting, basolateral targeting in polarized cells, and SV targeting (Blagoveshchenskaya et al., 1999; Hunziker and Fumey, 1994; Kirchhausen et al., 1997; Sandoval and Bakke, 1994). Indeed, dileucine motifs can even mediate several distinct trafficking events for a single protein. Their versatility appears to derive from their

ability to interact with multiple cytoplasmic clathrin adaptor protein (AP) complexes, including AP-1, AP-2, and AP-3, each of which mediates different protein sorting events and has a distinct subcellular localization (Heilker et al., 1996; Honing et al., 1998; Kirchhausen et al., 1997; Odorizzi et al., 1998; Rapoport et al., 1998). AP-1 is found at the TGN and mediates endosomal/lysosomal sorting, while AP-2 facilitates clathrin-mediated endocytosis at the plasma membrane (Heilker et al., 1996; Kirchhausen et al., 1997). AP-3 has been implicated in lysosomal targeting as well as SV budding from endosomes (Faundez et al., 1998; Odorizzi et al., 1998).

Chapter 3 describes the function of the VMAT2 dileucine-like sequence **KEEKMAIL**. Previous work in the laboratory showed that the isoleucine-leucine (IL) signal in this motif is necessary for VMAT2 endocytosis (Tan et al., 1998). This chapter demonstrates that the **KEEKMAIL** sequence, particularly the IL signal and the two upstream glutamates, targets VMAT2 to LDCVs. Replacement of the IL signal or the glutamates with alanine redirects VMAT2 from LDCVs into the constitutive secretory pathway. Thus, these residues are required for the proper targeting of VMAT2 into LDCVs (the regulated secretory pathway). This work, like that in the previous chapter, also demonstrates a novel and important role for a common protein trafficking motif.

CHAPTER 2

An Acidic Motif Retains Vesicular Monoamine Transporter 2 on Large Dense Core Vesicles

(reproduced from **The Journal of Cell Biology**, 2001, Vol. 152, pp. 1159-1168 by

copyright permission of The Rockefeller University Press)

Abstract

The release of biogenic amines from large dense core vesicles (LDCVs) depends on localization of the vesicular monoamine transporter VMAT2 to LDCVs. We now find that a cluster of acidic residues including two serines phosphorylated by casein kinase 2 is required for the localization of VMAT2 to LDCVs. Deletion of the acidic cluster promotes the removal of VMAT2 from LDCVs during their maturation. The motif thus acts as a signal for retention on LDCVs. In addition, replacement of the serines by glutamate to mimic phosphorylation promotes the removal of VMAT2 from LDCVs, whereas replacement by alanine to prevent phosphorylation decreases removal. Phosphorylation of the acidic cluster thus appears to reduce the localization of VMAT2 to LDCVs by inactivating a retention mechanism.

Introduction

Neurotransmitter release involves the regulated exocytosis of multiple, distinct types of secretory vesicle including synaptic vesicles (SVs) and large dense core vesicles (LDCVs). Although SVs and LDCVs both undergo regulated exocytosis, they differ in the site and mode of release, as well as in their contents. SVs cluster at the nerve terminal, mediate the rapid release of neurotransmitter into the synaptic cleft, and store classical neurotransmitter (Calakos and Scheller, 1996; Sudhof, 1995). In contrast, LDCVs appear in dendrites as well as axons, release their contents more slowly and in response to different stimuli than SVs, and contain neuromodulatory peptides, growth factors, and certain classical transmitters such as monoamines (De Camilli and Jahn, 1990; Martin, 1994). SVs and LDCVs also differ in their biogenesis. SVs form locally at the nerve terminal, whereas LDCVs bud directly from the *trans*-Golgi network (TGN) (Kelly and Grote, 1993; Tooze et al., 1993). Differences in protein sorting at these sites presumably underlie the differences in protein composition and hence vesicle function. However, little is known about the cellular mechanisms that target proteins to different classes of neurosecretory vesicles. To identify the signals that target proteins to SVs and LDCVs, we have focused on a family of membrane proteins required for the exocytotic release of neurotransmitter.

Classical transmitters are synthesized in the cytoplasm and require packaging into secretory vesicles by specific transport proteins. The localization of these proteins to

SVs, LDCVs or other types of neurosecretory vesicle determines the site of neurotransmitter storage and hence the mode of release. Dopamine in particular undergoes release from the cell body and dendrites of midbrain dopamine neurons as well as from nerve terminals in the striatum (Cheramy et al., 1981; Geffen et al., 1976; Heeringa and Abercrombie, 1995; Jaffe et al., 1998; Robertson et al., 1991), and somatodendritic release has been proposed to regulate neuronal activity (Aghajanian and Bunney, 1974; Grace and Bunney, 1995). Consistent with the release of dopamine at these sites, the vesicular monoamine transporter (VMAT2) responsible for dopamine transport into secretory vesicles resides on LDCVs and tubulovesicular structures in the cell body and dendrites as well as on SVs at the nerve terminal [Peter, 1995 #591; Weihe, 1994 #1043; Nirenberg, 1995 #602; Nirenberg, 1996 #858; Nirenberg, 1997 #894]. Studies of leech Retzius neurons further support the release of serotonin from both LDCVs located in the cell body and terminal and from SVs restricted to the terminal (Bruns and Jahn, 1995). Since the localization of VMAT2 to LDCVs influences the site and mode of monoamine release, the expression of VMAT2 on LDCVs presumably contributes to the role of dopamine, norepinephrine and serotonin in neuromodulation.

As an integral membrane protein, VMAT2 must also contain signals that direct its trafficking to LDCVs (Krantz et al., 2000). To identify the signals responsible for the membrane trafficking of VMAT2, we have used heterologous expression in PC12 cells, where VMAT2 targets preferentially to LDCVs (Krantz et al., 2000; Liu et al., 1994;

Varoqui and Erickson, 1998). We previously identified a dileucine-like motif in the cytoplasmic C-terminus of VMAT2 that mediates internalization from the plasma membrane (Tan et al., 1998). The closely related vesicular acetylcholine transporter (VACHT) contains a very similar motif, but unlike VMAT2, VACHT targets preferentially to synaptic-like microvesicles (SLMVs) rather than LDCVs in PC12 cells (Liu and Edwards, 1997a; Varoqui and Erickson, 1998). VMAT2 also differs from VACHT 4 and 5 residues upstream of the dileucine-like signal, positions shown to be important for the trafficking of other proteins (Dietrich et al., 1997; Pond et al., 1995). Although these residues do not affect the endocytosis of either VMAT2 or VACHT (Tan et al., 1998), we have recently found that they influence targeting to LDCVs and account in part for the observed differences in steady-state localization between these two transport proteins (Krantz et al., 2000).

The analysis of C-terminal deletions in VMAT2 now implicates an acidic motif containing two serines phosphorylated by casein kinase 2 (CK2) (Krantz et al., 1997) in targeting to LDCVs. After budding from the TGN, LDCVs undergo a maturation process in which proteins destined for other compartments such as lysosomes are removed (Klumperman et al., 1998; Kuliawat et al., 1997; Tooze et al., 1993). Deletion of the C-terminal acidic motif reduces the expression of VMAT2 on LDCVs by promoting its removal during LDCV maturation. The motif thus appears to act as a signal for retention on LDCVs. Interestingly, the TGN endoprotease furin contains a similar acidic cluster

with two serines phosphorylated by CK2. Phosphorylation of this motif increases furin retrieval from LDCVs (Dittie et al., 1997; Jones et al., 1995), apparently through an interaction with the novel cytosolic adaptor protein PACS-1 (phosphofurin acidic cluster sorting protein 1) (Wan et al., 1998). In VMAT2, replacement of serines in the acidic motif by aspartate to mimic phosphorylation also promotes the removal of VMAT2 during LDCV maturation, whereas replacement by alanine to prevent phosphorylation increases localization to LDCVs. Phosphorylation thus appears to promote VMAT2 retrieval from immature LDCVs by blocking the role of the acidic motif in retention. Very similar to furin, the phosphorylated form of the acidic cluster in VMAT2 also binds to PACS-1. Despite the similarities between VMAT2 and furin, however, VMAT2 normally resides in LDCVs whereas furin localizes to the TGN (Krantz et al., 2000; Liu and Edwards, 1997a). Differences in phosphorylation state presumably account for the divergent steady-state location of these proteins by influencing their removal from LDCVs.

Materials and Methods

Antibodies. Mouse monoclonal HA.11 antibody was obtained from Covance, the rat monoclonal HA antibody from Boehringer Mannheim, the rabbit polyclonal antiserum to secretogranin II from BioDesign, the mouse monoclonal antibody to the transferrin receptor from Zymed, the rabbit polyclonal antiserum to rab5 from Quality Controlled Biochemicals, the mouse monoclonal antibody to γ -adaptin from Transduction Laboratories, the rabbit polyclonal antibody to synaptophysin from Zymed, and the mouse monoclonal anti-his and goat polyclonal anti-GST antibodies from Amersham-Pharmacia. Secondary antibodies conjugated to FITC, Texas Red, Cy3, and Cy5 were obtained from Jackson ImmunoResearch Laboratories, and secondary antibodies conjugated to horseradish peroxidase from Amersham (anti-rabbit and anti-mouse) or Sigma (anti-goat). Brefeldin A was obtained from Epicentre Technologies. Drs. F. Brodsky and K. Mostov generously provided antibodies to TGN-38 and mannose-6-phosphate receptor, respectively.

Mutagenesis, Cell Culture and Immunofluorescence. Mutagenesis was performed using the Kunkel method (Kunkel et al., 1991). PC12 cells were transfected by electroporation, and independent cell clones isolated as previously described (Krantz et al., 2000). After plating onto glass coverslips coated with poly-L-lysine and Matrigel (Becton Dickinson) and treatment with 50 ng/ml NGF for 2-3 days, the cells were immunostained as

previously described (Tan et al., 1998) and visualized by confocal laser microscopy. For the experiments with brefeldin A (BFA), the cells were incubated with 5 $\mu\text{g/ml}$ BFA in standard medium for 15 minutes at 37°C before fixation.

Density gradient fractionation. PC12 cells were rinsed with calcium/magnesium-free phosphate-buffered saline (cmf-PBS), harvested in 0.3 M sucrose, 10 mM Hepes pH 7.4 (sucrose-Hepes buffer) containing 2 mM Mg EGTA, 1 $\mu\text{g/ml}$ leupeptin, 1 $\mu\text{g/ml}$ pepstatin, and 10 $\mu\text{g/ml}$ PMSF, and the cells disrupted at a clearance of 10 μm in a ball-bearing homogenizer. After pelleting the nuclei at 1000 g for 8 minutes, the resulting post-nuclear supernatant (PNS) was layered onto a linear 0.6-1.6 M sucrose gradient and sedimented to equilibrium at 30,000 rpm for 12-16 hours in an SW41 rotor at 4°C. Fractions were collected from the top.

Velocity gradient sedimentation. Metabolic labeling with ^{35}S -sulfate was done as done previously described (Dittie et al., 1996; Tooze and Huttner, 1990). Briefly, PC12 cells were rinsed twice with sulfate-free medium, incubated at 37°C for 30 minutes, then labeled for 5 minutes in the same medium containing 0.5 mCi/ml ^{35}S -sulfate (NEN). To label SgII in the TGN, the cells were then chilled and harvested. To allow labeled SgII to enter iLDCVs, the labeled cells were incubated at 37°C for an additional 15 minutes in standard PC12 medium containing sulfate. To allow the passage of labeled SgII into

mature LDCVs, cells were incubated for 6 hours with 0.2 mCi/ml ³⁵S-sulfate in sulfate-free medium, then for 12-16 hours in standard PC12 medium.

Gradients were performed according to established protocols (Blagoveshchenskaya et al., 1999; Dittie et al., 1996). After labeling with ³⁵S-sulfate, cells were immediately placed on ice, rinsed with cold cmf-PBS containing 1 mM MgSO₄, harvested in a modified sucrose-Hepes buffer (0.25 M sucrose, 10 mM Hepes-KOH at pH 7.2) containing protease inhibitors, 1 mM EGTA, and 1 mM MgSO₄, the PNS prepared as above, layered onto a linear 0.3 -1.2 M sucrose gradient in 10 mM Hepes-KOH, pH 7.2 and sedimented for 19 minutes at 25,000 rpm in an SW41 rotor at 4° C.

To separate iLDCVs from mLDCVs, fractions from the velocity gradient that contained iLDCVs or mLDCVs were identified by scintillation counting, pooled, diluted with 10 mM Hepes-KOH pH 7.2, layered onto linear 0.9-1.7 M sucrose gradients made in 10 mM Hepes-KOH pH 7.2 and sedimented for 21 hours at 30,000 rpm in an SW41 rotor at 4° C. Fractions were collected from the top.

Western analysis and quantitation. Proteins were separated by electrophoresis through SDS-polyacrylamide, electroblotted to PVDF or nitrocellulose and immunostained as previously described (Krantz et al., 2000). After detection of the bound antibodies using

SuperSignal West Pico substrate (Pierce), the films were optically scanned, digitized and quantified using NIH Image.

To quantify the one-step sucrose equilibrium gradients, the amount of HA or SgII immunoreactivity in each gradient fraction was expressed as a fraction of the total HA or SgII immunoreactivity in all gradient fractions. For the two-step gradients, the sorting index for localization to i- or m-LDCVs was determined by first identifying the 2 peak iLDCV fractions and the 2 peak mLDCV fractions through autoradiography for ³⁵S-sulfate labeled SgII. The HA immunoreactivity in these peak fractions was then measured by densitometry, and used to calculate the proportion of HA immunoreactivity in the 2 peak iLDCV fractions and the 2 peak mLDCV fractions relative to the total HA immunoreactivity in all 4 peak fractions.

Bacterial expression and in vitro phosphorylation. C-terminal fragments of the wild type, 507*, AA, and DD VMAT2 cDNAs were subcloned using EcoRV, inserted in-frame into the SmaI site of pGEX-3X-1 (Pharmacia) and expressed as GST fusion proteins in *E.coli* as previously described (Krantz et al., 2000). The furin-binding domain of PACS-1 subcloned into pET-16b (Novagen) was also expressed and purified by Ni²⁺ chromatography. To phosphorylate the GST fusions, the proteins bound to glutathione-Sepharose beads were incubated in 20 mM Tris pH 7.5, 50 mM KCl, 1 mM DTT, and 10 mM MgCl₂ (phosphorylation buffer) containing 200 μM ATP, 500 μCi/μmol γ-³²P-ATP,

and 250 U casein kinase 2 for 90 min at 30°C, washed twice in PBS with 15 mM EDTA, and tested for binding to PACS-1.

PACS-1 binding assay. Following a procedure described previously (Xiang et al., 2000), GST fusion proteins were bound to glutathione-Sepharose beads for a final concentration of ~5 µg/ml, incubated in 150 mM NaCl, 50 mM Tris pH 7.5, 2 mM MgCl₂, and 2% Triton X-100 (binding buffer) with 2.5 µg/ml purified PACS-1 for 1 hour at room temperature, washed three times in binding buffer, and the proteins eluted with SDS sample buffer, separated by electrophoresis, and transferred to PVDF. Phosphorylated GST fusions were detected by autoradiography, and unlabeled GST fusions and bound PACS-1 were detected by Western analysis using anti-GST and anti-His antibodies, respectively. After autoradiography or detection of the bound antibodies by ECL Plus (Amersham-Pharmacia), the films were optically scanned.

Results

Deletion of an Acidic Motif Redistributes VMAT2 Away from LDCVs

To identify signals that influence the subcellular location of VMAT2, we expressed a series of C-terminal truncations in PC12 cells, which produce both LDCVs and SLMVs. These constructs contain an HA epitope in the luminal loop between transmembrane domains 1 and 2, and stop codons after residues 507, 491, and 484 (507*, 491* and 484*) (Fig. 1A). Using immunofluorescence to compare the localization of the introduced VMAT2 with secretogranin II (SgII), a soluble protein contained in LDCVs, we found that wild type VMAT2 colocalizes precisely with SgII at the tips of processes (Fig. 1B, a-c). Both proteins are expressed at low levels in cell bodies. In contrast, the deletion mutants colocalize poorly with SgII (Fig. 1B, d-l). These truncations exhibit a perinuclear staining pattern with little expression at the tips of processes, indicating the presence of a second trafficking motif at the C-terminus of VMAT2. The distribution of 507* strongly resembles that of 491* and 484*, indicating that the last eight amino acids of VMAT2 (DDEESESD) comprise a major trafficking signal.

To confirm that deletion of the acidic cluster alters the localization of VMAT2 in PC12 cells, we analyzed the 507* mutant by density gradient fractionation. Equilibrium sedimentation through sucrose, which separates LDCVs from lighter membranes such as SLMVs and endosomes, shows that wild type VMAT2 colocalizes with SgII in heavy, LDCV-containing fractions (Fig. 2A), as previously observed (Krantz et al., 2000). Only

very small amounts of VMAT2 appear in lighter fractions (Fig. 2A). In contrast, the 507* mutant colocalizes less well with SgII in heavy fractions and is more prominent in lighter fractions (Fig. 2B). Equilibrium sedimentation thus confirms the importance of a C-terminal acidic cluster for the localization of VMAT2 to LDCVs.

By immunofluorescence, the 507* mutant localizes to a perinuclear compartment. To identify this compartment, we used double staining to assess the colocalization of 507* with markers for various intracellular membranes. The 507* mutant does not colocalize with markers for the endoplasmic reticulum (ribophorin II), cis-Golgi (β -COP), or early endosomes (rab 5) (data not shown). The sucrose density gradient suggested expression on lighter membranes that might represent SLMVs (Fig. 2B), but 507* shows only partial colocalization with synaptophysin (Fig. 3, a-c). The perinuclear distribution of 507* resembles that of the endosomal transferrin receptor (TfR), the late endosomal mannose 6 phosphate receptor (M6PR) (Fig. 3, d-i) and the lysosomal cathepsin B (data not shown). However, the merged images at higher magnification show only minor colocalization. On the other hand, 507* colocalizes more extensively with markers for the trans-Golgi network (TGN) such as the clathrin adaptor protein AP-1 (data not shown) and TGN-38 (Fig. 3, j-l).

Localization of 507* to Immature LDCVs

To determine whether 507* localizes to the TGN or to closely apposed membranes, we treated the stable PC12 transformants with brefeldin A (BFA), a fungal derivative that causes fragmentation of the TGN. If expressed in the TGN, 507* should redistribute to the cell periphery after exposure to BFA. BFA indeed collapses TGN-38 as expected, but 507* remains largely perinuclear (Fig. 4A). Since immature LDCVs (iLDCVs) bud from the TGN and may function as a specialized extension of this sorting compartment, 507* might localize instead to iLDCVs. To test this possibility, we used sulfate labeling of SgII together with gradient fractionation (Tooze and Huttner, 1990). Cells were labeled first for 5 minutes with ³⁵S-sulfate, which incorporates heavily into SgII as it transits the TGN, then either chilled on ice to prevent the exit of labeled SgII from the TGN, or incubated at 37°C in medium with unlabeled sulfate for an additional 15 minutes to allow passage of the labeled SgII into iLDCVs. Chase for 15 minutes does not allow sufficient time for LDCV maturation. We then used velocity gradient fractionation to separate iLDCVs from the TGN. Autoradiography showed the shift of SgII from heavy to light fractions over the 15 minute chase (Fig. 4B), as expected. Western analysis showed that 507* colocalizes with the iLDCV-containing rather than the TGN-containing fractions (Fig. 4B). Thus, 507* may reside on iLDCVs even though it is greatly reduced on the entire population of LDCVs (Figs. 1, 2).

The presence of 507* on iLDCVs despite a low proportion on LDCVs raises the possibility that the mutant is removed during LDCV maturation. To determine whether

507* indeed resides on iLDCVs, we again used the labeling of SgII with ³⁵S-sulfate followed by gradient fractionation (Blagoveshchenskaya et al., 1999; Dittie et al., 1997). Labeling for 5 minutes followed by incubation for an additional 15 minutes with unlabeled sulfate allows the labeled SgII to enter iLDCVs but not mature LDCVs (mLDCVs). Labeling for 6 hours followed by 12 hours of chase allows sufficient time for the maturation of LDCVs containing labeled SgII. To separate iLDCVs from mLDCVs and hence determine the fate of VMAT2 during LDCV maturation, we used sequential velocity and equilibrium sedimentation through sucrose. Autoradiography for ³⁵S-labeled SgII identified the fractions containing either iLDCVs or mLDCVs, and Western blotting identified those that contain VMAT2. Wild type VMAT2 colocalizes with labeled SgII in both i- and m-LDCV fractions (Fig. 5A, B). In contrast, 507* is barely detectable in mLDCV-containing fractions but colocalizes with labeled SgII in iLDCV-containing gradient fractions (Fig. 5A,B). These iLDCV fractions do not contain detectable amounts of other membranes including endosomes and SLMVs (Fig. 5B), enabling us to distinguish between the VMAT2 on iLDCVs and on other membranes. To quantify these observations, we studied three stable cell lines each for wild type and 507* VMAT2, and compared the amounts of protein on i- and m-LDCVs. Using autoradiography to identify the peak iLDCV and mLDCV fractions, we determined the amount of VMAT2 in these fractions by densitometry and expressed the amount in either iLDCVs or mLDCVs as a fraction of total VMAT2 in all peak fractions. The analysis

shows that more than half of wild type VMAT2 in LDCVs localizes to mLDCVs, whereas only a small fraction (~10%) of 507* resides on these membranes (Fig. 5C). In contrast, a substantially larger proportion of 507* localizes to iLDCVs relative to wild type VMAT2. The quantitation of iLDCVs specifically excludes VMAT2 that does not cofractionate with the peak of SgII, focusing specifically on the protein in iLDCVs rather than that in endosomes or SLMVs. A substantial proportion of the 507* that enters the regulated secretory pathway thus appears to be removed from LDCVs during maturation, indicating a role for the acidic cluster in retention on mLDCVs.

The Role of Phosphorylation in VMAT2 Removal from Maturing LDCVs

Phosphorylation of the acidic cluster in VMAT2 may also influence targeting to LDCVs. In the case of furin, replacement of phosphorylated serines within the cluster by aspartate to mimic phosphorylation promotes retrieval from LDCVs to the TGN. In contrast, replacement of these serines by alanine to prevent phosphorylation promotes localization to LDCVs (Dittie et al., 1997; Jones et al., 1995). Since serines within the acidic cluster of VMAT2 also undergo phosphorylation by casein kinase 2 (Krantz et al., 1997), we investigated the role of phosphorylation in VMAT2 trafficking to LDCVs by replacing the serines with either alanine (AA mutant) or aspartate (DD mutant). After stable expression of the two constructs in PC12 cells, we compared their localization to SgII by immunofluorescence and density gradient fractionation. Like wild-type VMAT2, the AA

mutant colocalizes extensively with SgII at the tips of neuritic processes, and appears at low levels in the cell body (Fig. 6, a-c). By gradient fractionation as well, wild type and AA VMAT2 colocalize with SgII (Fig. 7B). The DD mutant also colocalizes with SgII at the tips of processes and in heavy gradient fractions (Fig. 6, d-f, Fig. 7C), but a significant proportion does not colocalize with SgII. Rather, DD appears partially redistributed to a perinuclear compartment by immunofluorescence and to membranes lighter than LDCVs by gradient fractionation (Fig. 6, d-f, Fig. 7C).

Localization of the DD mutant resembles that observed for 507*, suggesting that DD may also undergo removal from LDCVs. To address this possibility, we used the two-step fractionation procedure to separate i- and m-LDCVs. By this analysis, the AA mutant strongly resembles wild type VMAT2, with more than half of the AA in the regulated secretory pathway appearing on mLDCVs (Fig. 5C). In contrast, the localization of DD resembles that of 507*, with reduced expression on mLDCVs. Of the DD mutant sorted into LDCVs, only ~36% resides on mLDCVs (Fig. 5C). Although the effect of the DD mutation on localization to LDCVs appears less dramatic than that of the 507* deletion, the proportion of DD on mLDCVs is clearly reduced relative to AA (~64%) and wild type VMAT2 (~56%). Thus, phosphorylation of the acidic motif apparently influences the localization of VMAT2 to LDCVs by regulating the removal of VMAT2 during LDCV maturation.

Binding to PACS-1

The AA and DD mutations in VMAT2 have effects very similar to the analogous AA and DD mutations in furin. In both cases, replacement of the serines by aspartate to mimic phosphorylation promotes removal from iLDCVs, whereas replacement by alanine to mimic dephosphorylation promotes retention on LDCVs. However, VMAT2 normally resides on LDCVs whereas furin normally resides in the TGN [Molloy, 1994 #1044; Jones, 1995 #1040; Schafer, 1995 #995]. One possible explanation for this discrepancy is that the acidic clusters in the two proteins interact with distinct cytosolic sorting machinery.

The cytoplasmic protein PACS-1 is considered to mediate the retrieval of furin from LDCVs. PACS-1 binds to the phosphorylated acidic cluster in furin and appears to promote retrieval to the TGN through an interaction with the clathrin adaptor protein AP-1 (Wan et al., 1998). To determine whether VMAT2 also binds to PACS-1, we produced GST fusion proteins containing the C-termini of wild type, AA, DD, and 507* VMAT2, and examined binding to a bacterially expressed domain of PACS-1 known to interact with furin (Wan et al., 1998). We first compared PACS-1 binding to a GST fusion containing the C-terminus of wild type VMAT2 that either was or was not phosphorylated *in vitro* by casein kinase 2. Very similar to furin, PACS-1 binds more strongly to the phosphorylated than to the unphosphorylated form of VMAT2 (Fig. 8). In addition, VMAT2 binds PACS-1 with an avidity similar to furin, supporting the parallel

between VMAT2 and furin with respect to this interaction. We then compared PACS-1 binding by wild type, AA, and DD C-terminal VMAT2 domains. As anticipated, PACS-1 binds strongly to the C-terminus of the DD mutant and at very low levels to wild type VMAT2 and the other mutants (Fig. 8). Thus, PACS-1 binds specifically and preferentially to the phosphorylated acidic cluster in VMAT2.

Discussion

The analysis of serial C-terminal truncations shows that an acidic cluster at the distal C-terminus of VMAT2 influences localization to LDCVs. The sorting motif includes six acidic residues and two serines previously shown to be phosphorylated by casein kinase 2 (Krantz et al., 1997). By both immunofluorescence and gradient fractionation, deletion of these eight residues reduces VMAT2 expression on LDCVs. Phosphorylation of the acidic cluster apparently has a similar effect on steady-state localization of the transporter. Replacement of serines in the cluster by aspartate to mimic phosphorylation reduces localization of VMAT2 to LDCVs. In contrast, replacement of the serines with alanine to prevent phosphorylation does not perturb the localization of VMAT2 to LDCVs.

Phosphorylation of an acidic cluster in furin reduces LDCV expression by promoting removal during LDCV maturation, and dephosphorylation blocks removal (Dittie et al., 1997; Jones et al., 1995). We now show that the DD mutation reduces VMAT2 expression on m- but not iLDCVs, suggesting that phosphorylation also promotes VMAT2 removal during LDCV maturation. In contrast, the AA mutation which does not permit phosphorylation at these sites does not substantially affect the proportion of VMAT2 on m- versus iLDCVs. Thus, the data strongly suggest that phosphorylation of the acidic cluster reduces the localization of both VMAT2 and furin

on LDCVs by promoting their removal during LDCV maturation, whereas dephosphorylation promotes the retention of both proteins on LDCVs.

Although phosphorylation of an acidic cluster appears to promote the removal of both VMAT2 and furin from iLDCVs, VMAT2 normally localizes to LDCVs whereas furin localizes to the TGN. How can the same motif acting on the same trafficking event contribute to such divergent steady-state localization? The acidic clusters in the two proteins may interact with distinct sorting machinery. PACS-1 mediates the retrieval of furin by binding to the phosphorylated acidic cluster (Wan et al., 1998). Removal of VMAT2 from LDCVs may be mediated by a different PACS isoform or an entirely distinct protein interaction. However, we have found that PACS-1 binds to VMAT2 and furin with apparently similar avidity. Further, PACS-1 binds preferentially to the phosphorylated form of the acidic cluster in VMAT2, just as it does with furin.

Since the acidic motifs in VMAT2 and furin have similar effects on subcellular location, influence the same trafficking event and interact with the same sorting machinery, differences in the state of phosphorylation appear to account for the divergent steady-state localization of these two proteins. Phosphorylation by CK2 is often constitutive; however, dephosphorylation of the acidic cluster in furin has been shown to undergo regulation. Indeed, dephosphorylation by a specific isoform of protein phosphatase 2A regulates the endocytic trafficking of furin (Molloy et al., 1998). Our results now indicate that, just as the persistent phosphorylation of furin in LDCVs

promotes its retrieval to the TGN, dephosphorylation of the acidic cluster in VMAT2 appears to promote its retention on mLDCVs.

Previous work has suggested that PACS-1 mediates the retrieval of furin from iLDCVs to the TGN. Consistent with a role for retrieval in the steady-state localization of furin to the TGN, reduction of PACS-1 expression redistributes furin out of the TGN (Wan et al., 1998). In addition, PACS-1 links furin to AP-1, a component of the clathrin sorting machinery, and AP-1-dependent retrieval from iLDCVs has been observed for several proteins, including the mannose-6-phosphate receptor (Klumperman et al., 1998). We now show that VMAT2 also binds to PACS-1. However, the 507* mutant undergoes retrieval from LDCVs even though it lacks the acidic cluster and hence cannot interact with PACS-1. Indeed, 507* is excluded from mLDCVs to an even greater extent than the DD mutant, which strongly binds PACS-1. Deletion of the acidic cluster in furin redistributes the protein into endosomes but may not eliminate expression in the TGN (Schafer et al., 1995), suggesting that the motif may not be essential for retrieval from LDCVs. Thus, rather than promoting retrieval, the acidic cluster appears to function as a retention signal that prevents the removal of proteins from LDCVs. Phosphorylation by casein kinase 2 and subsequent binding to PACS-1 presumably inhibit this retention signal and hence promote removal. Conversely, regulated dephosphorylation restores the function of the acidic cluster as a retention signal. Removal from LDCVs may therefore represent a default pathway blocked by the acidic cluster in its dephosphorylated state.

Where do the VMAT2 mutants (507* and DD) go after removal from maturing LDCVs? Although the velocity gradient suggests little expression in the TGN (Fig. 4), the immunofluorescence shows colocalization with TGN38 and to a lesser extent with the late endosomal and lysosomal proteins M6PR and cathepsin B. The mutants may therefore cycle repeatedly between the TGN and iLDCVs, increasing the likelihood of diversion to late endosomes and lysosomes. Supporting this possibility, we have observed increased turnover of 507* ($t_{1/2}$ ~4 hours) relative to wild type VMAT2 ($t_{1/2}$ ~7 hours). Alternatively, the removal of 507* and DD mutants from maturing LDCVs might increase their trafficking to the constitutive secretory pathway and hence to SLMVs. Immunofluorescence and gradient fractionation indicate some colocalization of 507* with synaptophysin (Figs. 3a-c and 5B). However, we have not observed any increased expression of these mutants on SLMVs separated from other membrane vesicles by glycerol velocity gradient fractionation (Clift-O'Grady et al., 1990) (D.E.K., C.W., R.H.E., unpublished observations). In addition, we have not detected the constitutive delivery of 507* and DD mutants to the cell surface (data not shown). In contrast to mutants defective in sorting to the regulated secretory pathway, which internalize large amounts of HA antibody from the medium due to their external HA epitope and their constitutive delivery at the cell surface (C.W., R.H.E., in preparation), wild type, 507*, DD and AA VMAT2 exhibit very little uptake of the HA antibody. Thus, the C-terminal

acidic cluster appears to have little role in sorting to the regulated secretory pathway in the TGN.

Since acidic residues upstream of the IL motif in VMAT2 also contribute to localization on LDCVs, what is the relationship between these residues and the more C-terminal acidic cluster? The two motifs may both be required for retention on LDCVs. However, acidic residues upstream of the dileucine motif in other proteins have been shown to promote internalization from the plasma membrane (Dietrich et al., 1997; Pond et al., 1995), suggesting that these residues would more likely promote than to inhibit VMAT2 removal from LDCVs. Alternatively, the two glutamates upstream of the dileucine-like motif may be required for another trafficking event such as sorting in endosomes or the TGN.

VMAT2 sorts to synaptic vesicles and tubulovesicular structures as well as LDCVs (Nirenberg et al., 1996; Nirenberg et al., 1997; Nirenberg et al., 1995), indicating the potential of acidic cluster phosphorylation to regulate the proportion of protein on these different populations of neurosecretory vesicles. Since LDCVs reside in the cell body and dendrites as well as the nerve terminal, alterations in the expression of VMAT2 on LDCVs have the potential to affect somatodendritic release. LDCVs also differ from SVs and other secretory vesicles in their responsiveness to different stimuli, and in the rate of release (Bruns and Jahn, 1995). The regulation of VMAT2 phosphorylation on its

acidic cluster may thus influence the site, mode and hence the role of monoamines in signalling.

In summary, VMAT2 resembles furin with respect to the influence of phosphorylation on membrane trafficking and on binding to PACS-1, but VMAT2 differs in steady-state location. Differences in phosphorylation state apparently confer the differences in subcellular distribution by regulating removal from LDCVs. In addition, the acidic motif in VMAT2 acts as a retention signal that is inactivated by phosphorylation, rather than as a positive signal for removal from LDCVs. The motif may thus interact in its unphosphorylated state with a protein that retains VMAT2 on LDCVs. Phosphorylation may displace this protein, promoting an interaction with PACS and removal from LDCVs. A large number of membrane proteins including the synaptic vesicle protein synaptotagmin as well as furin and VMAT2 contain acidic motifs phosphorylated by casein kinase [Bennett, 1993 #550; Molloy, 1999 #1046]. The mechanism of regulated retention may therefore act at multiple trafficking events to influence the subcellular distribution and physiological role of many proteins.

Figures

Figure 1. Analysis of C-terminal VMAT2 deletions by immunofluorescence

(A) Serial deletions of the VMAT2 C-terminus were created by inserting stop codons after residues 507, 491 and 484. The asterisk (*) indicates the position of the inserted stop codon.

(B) PC12 cells stably expressing HA-tagged wild type VMAT2 or the deletion mutants were double-stained with a mouse monoclonal antibody to HA followed by anti-mouse antibodies conjugated to Cy3 (a, d, g, j), and with a polyclonal rabbit antiserum to SgII followed by anti-rabbit antibodies conjugated to Cy5 (b, e, h, k), then examined by confocal microscopy. Merged Cy3 and Cy5 images are shown in c, f, i, and l. Wild-type VMAT2 (a-c) colocalizes extensively with SgII and appears primarily at the tips of cell processes (marked by arrows). In contrast, the mutants show little colocalization with SgII (d-l). All exhibit reduced staining at the tips of process and strong expression in the perinuclear region (marked by arrowheads). The bar indicates 10 μm .

A

wt —PPAKEEKMAILMDHNCPIKTKMYTQNNVQSYPIGDDEESED
507* —PPAKEEKMAILMDHNCPIKTKMYTQNNVQSYPIG*
491* —PPAKEEKMAILMDHNCPI*
484* —PPAKEEKMAIL*

B

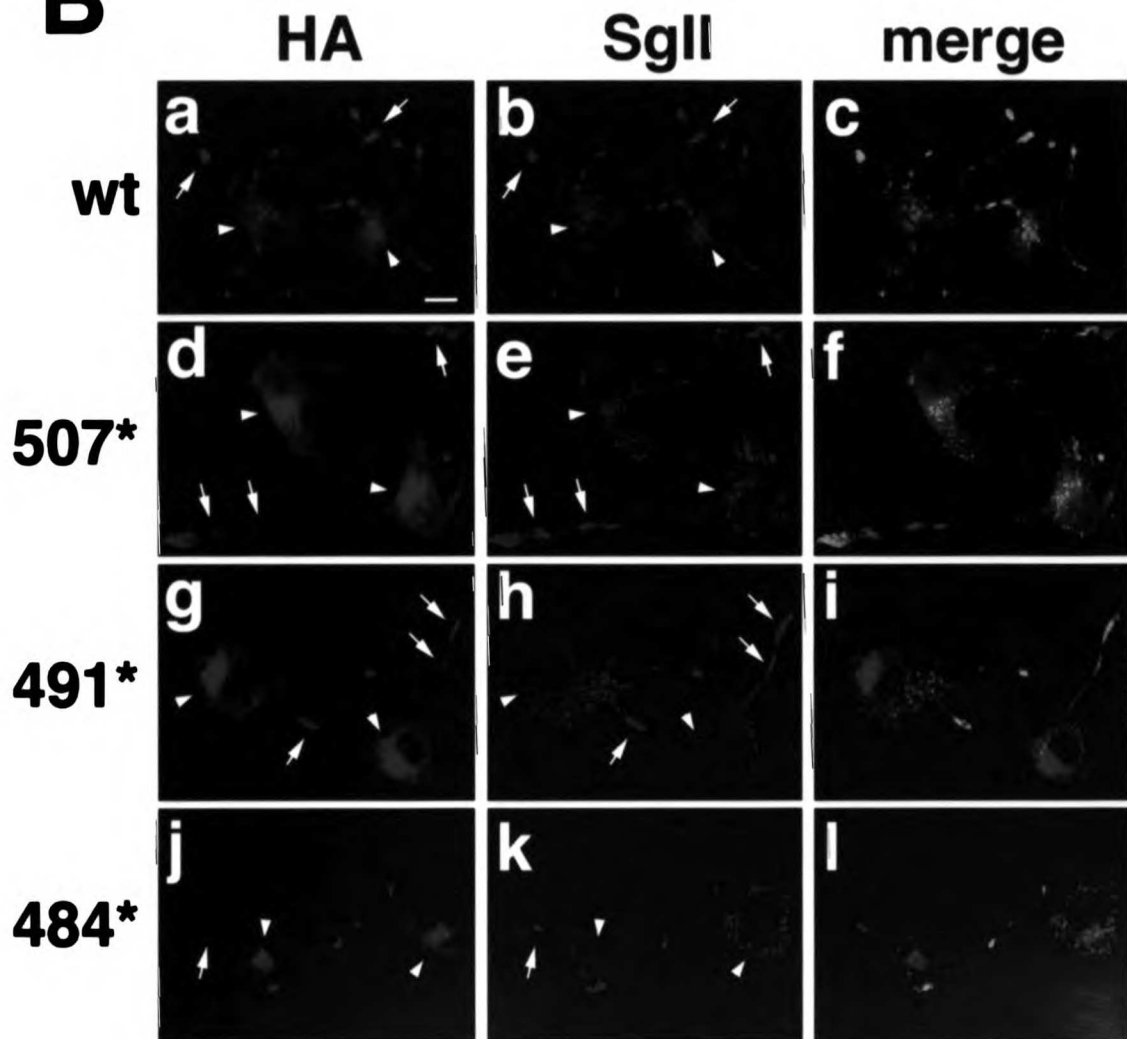


Figure 2. Density gradient fractionation of wild type and 507* VMAT2

Post-nuclear supernatants from PC12 cells stably expressing HA-tagged wild type (A) and 507* (B) VMAT2 were separated by equilibrium gradient centrifugation through 0.6-1.6 M sucrose. Fractions were collected and analyzed by Western blot using the monoclonal HA antibody to detect VMAT2 (upper panels in A and B), and a polyclonal antibody to detect the LDCV marker SgII (lower panels). The immunoblots were then digitized and quantified using NIH Image. For each fraction, the amount of VMAT2 and SgII is expressed as a percentage of total immunoreactivity in all the fractions. Wild type VMAT2 cofractionates with SgII in heavy fractions, whereas 507* cofractionates to a lesser extent with SgII and appears instead in lighter fractions. The analysis of three different stable cell lines for each construct yielded similar results.

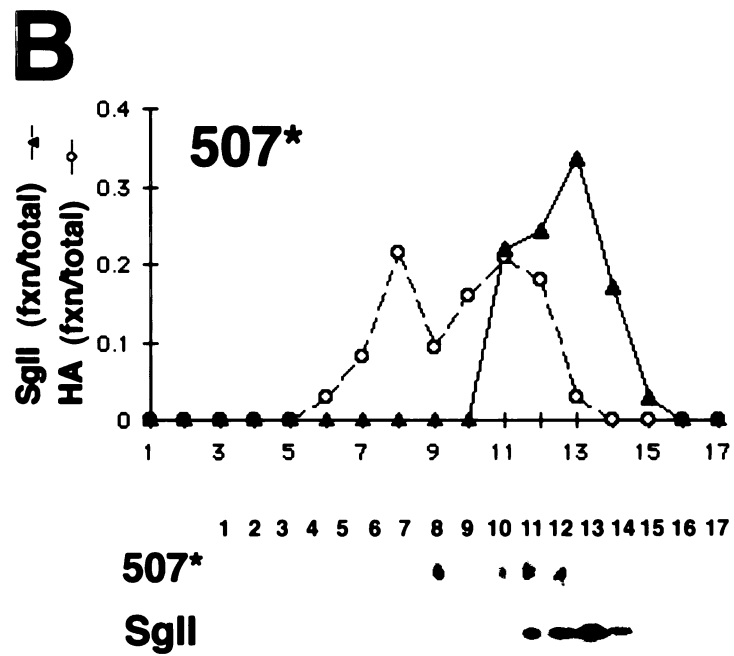
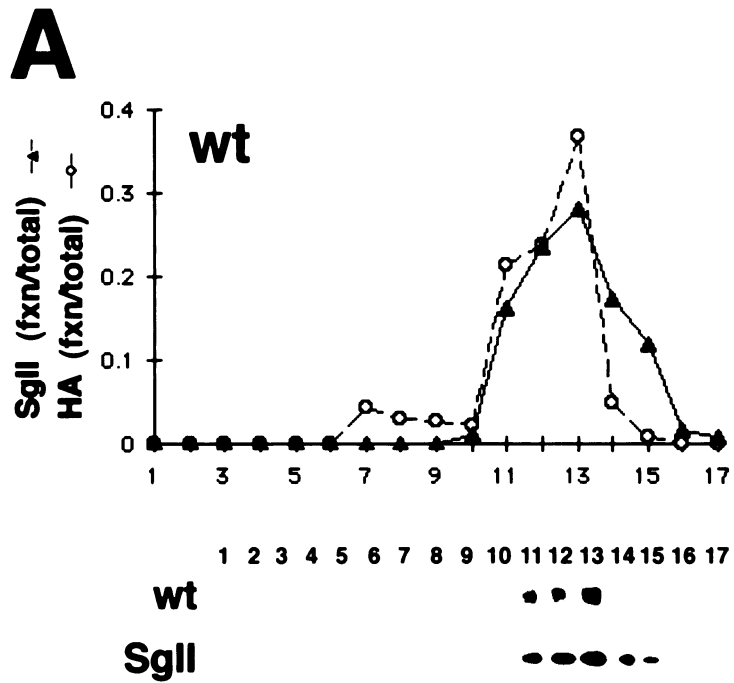


Figure 3. 507* colocalizes with TGN-38 by immunofluorescence

PC12 cells stably expressing 507* were double stained with the mouse monoclonal antibody to HA (b, h, k) and polyclonal antibodies to synaptophysin, mannose-6-phosphate receptor (M6PR), and TGN-38 (a, g, j), or with a rat monoclonal HA antibody (e) and a mouse monoclonal antibody to transferrin receptor (TfR) (d). Secondary antibodies conjugated to Cy3 and Cy5 were used to distinguish between 507* and the marker proteins, respectively. Merged Cy3 and Cy5 images are shown in c, f, i, and l. 507* does not colocalize with synaptophysin, TfR, or M6PR, but does colocalize extensively with TGN-38. Insets show the perinuclear staining (arrowheads) at high magnification. Bar, 10 μ m.

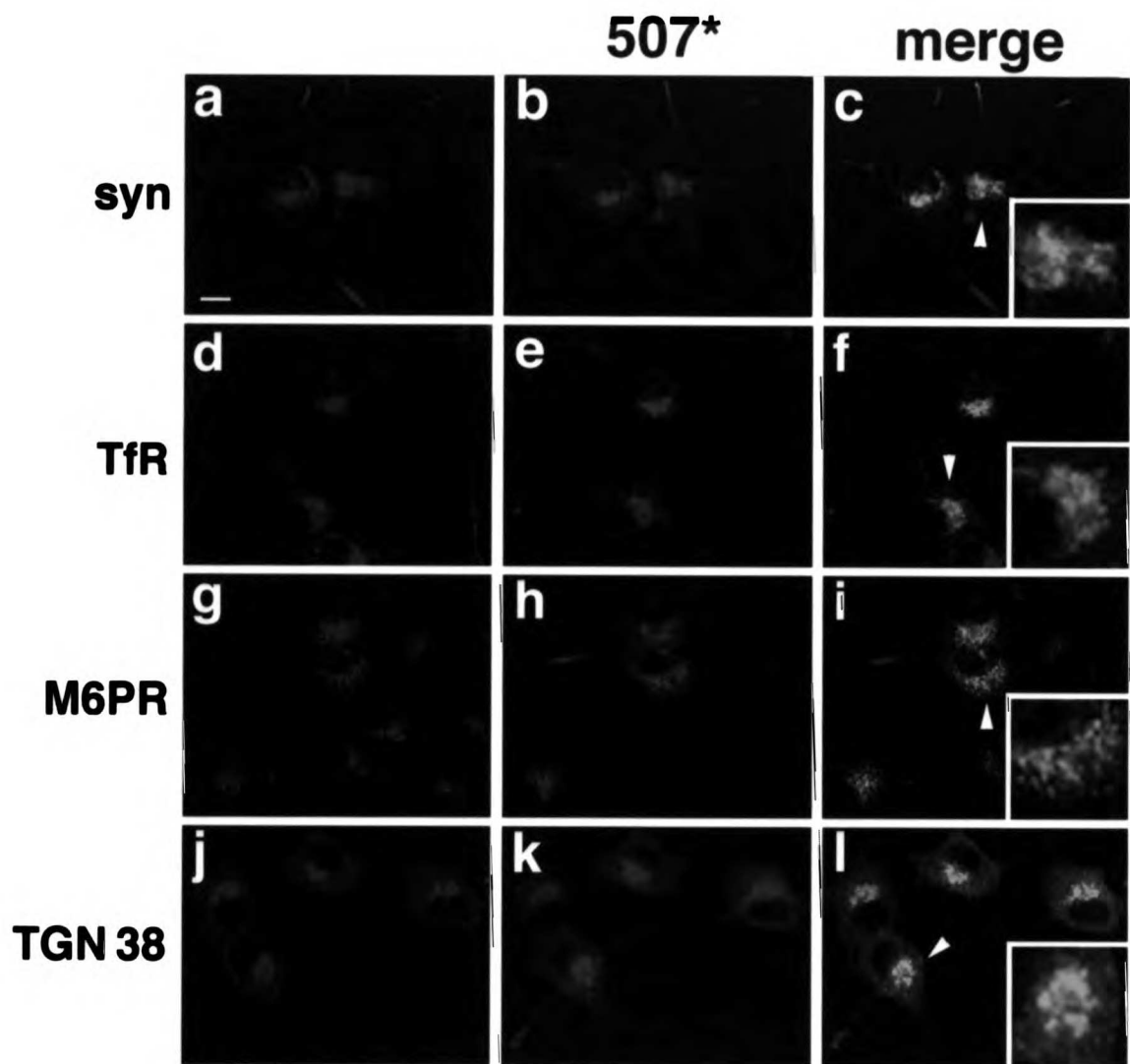


Figure 4. The 507* deletion localizes to a BFA-resistant compartment that cofractionates with iLDCVs

(A) PC12 cells stably expressing 507* were incubated without or with 5 $\mu\text{g/ml}$ brefeldin A (BFA) for 15 minutes, then double-stained with mouse monoclonal HA antibody and rabbit polyclonal TGN-38 antiserum followed by anti-mouse antibody conjugated to Cy3 and anti-rabbit antibody conjugated to Cy5. 507* and TGN-38 colocalize in the absence but not in the presence of BFA. As indicated by the dispersion of TGN-38, BFA causes fragmentation of the TGN but not the compartment containing 507*. Insets show the perinuclear staining (arrowheads) at high magnification. Bar, 10 μm .

(B) To label SgII in the TGN, cells were incubated for 5 minutes with 0.5 mCi/ml ^{35}S -sulfate, then chilled on ice. To allow the labeled SgII to enter iLDCVs, cells were labeled in the same way but incubated at 37°C for an additional 15 minutes in medium with unlabeled sulfate before harvesting. The resulting post-nuclear supernatants were then separated by velocity sedimentation through 0.3-1.2 M sucrose, and fractions collected from the top of the gradient. Labeled SgII was detected by autoradiography and 507* protein by Western analysis using the monoclonal HA antibody. 507* co-migrates with iLDCVs in fractions 2-4 rather than with the TGN in fractions 7-9.

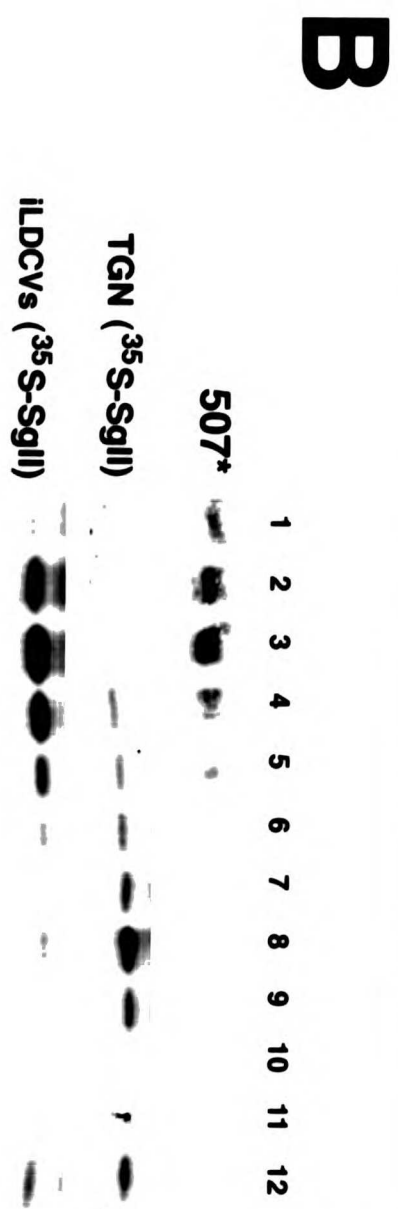
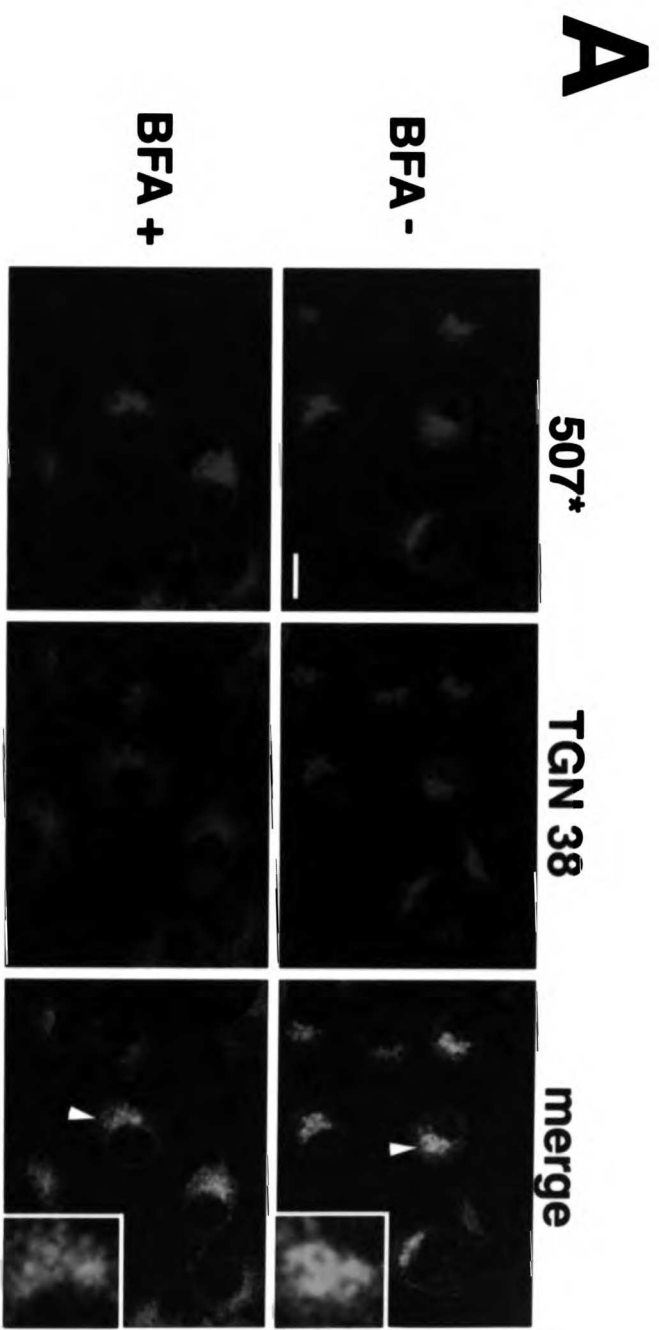


Figure 5. VMAT2 mutants 507* and DD localize preferentially to immature rather than mature LDCVs

(A) Cells were labeled with 0.2 mCi/ml ^{35}S -sulfate for 6 hours, incubated for an additional 12 hours with unlabeled sulfate, and post-nuclear supernatants (PNS) separated by velocity sedimentation through 0.3-1.2 M sucrose. Fractions containing mLDCVs were identified by scintillation counting, pooled, and further separated by equilibrium sedimentation through 0.9-1.7 M sucrose. The resulting fractions were collected from the top of the gradient and either submitted to autoradiography to detect radiolabeled SgII or subjected to Western analysis for HA to detect VMAT2. The starting material (PNS) is shown to the right of the fractions. Wild type VMAT2 cofractionates with labeled SgII in mLDCVs (fractions 9 and 10) and shows enrichment in these fractions relative to the PNS. 507* cofractionates with mLDCVs in fraction 9, but is not enriched relative to the PNS.

(B) Cells were labeled with 0.5 mCi/ml ^{35}S -sulfate for 5 minutes and incubated for an additional 15 minutes with unlabeled sulfate. After velocity sedimentation, the fractions containing iLDCVs were pooled and further separated by equilibrium sedimentation as described in A, followed by autoradiography for ^{35}S -sulfate, Western analysis for HA, γ -adaptn, TfR and synaptophysin. Both wild type and 507* VMAT2 cofractionate with labeled SgII in iLDCVs (fractions 7-8). Relative to the PNS, 507* is more enriched in

iLDCVs than mLDCVs (A). Light membranes such as endosomes and SLMVs do not contaminate the iLDCV fractions containing ^{35}S -SgII.

C) For wt, 507*, AA, and DD VMAT2, three stable cell lines were subjected to the two-step fractionation procedure described above. Peak iLDCV and mLDCV fractions were identified by autoradiography, and the amount of VMAT2 protein in these fractions was measured using NIH Image. The amount of protein on iLDCVs and mLDCVs is expressed as a fraction of the total VMAT2 immunoreactivity in all peak fractions. Only the two peak LDCV fractions containing ^{35}S -SgII were used to determine the amount of VMAT2 expressed on i or mLDCVs. The bars indicate the mean \pm standard error (n=3).

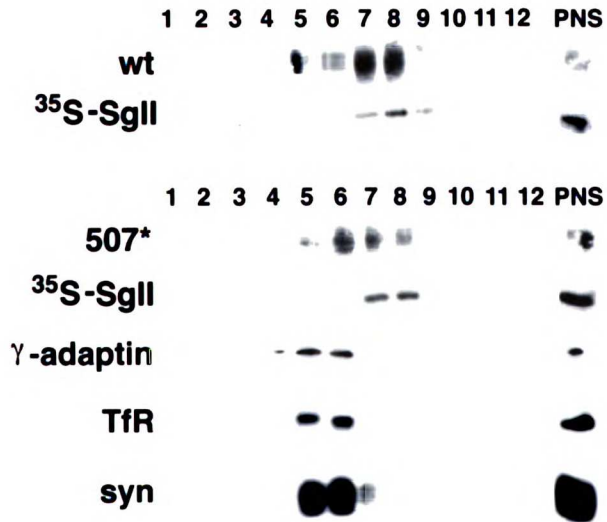
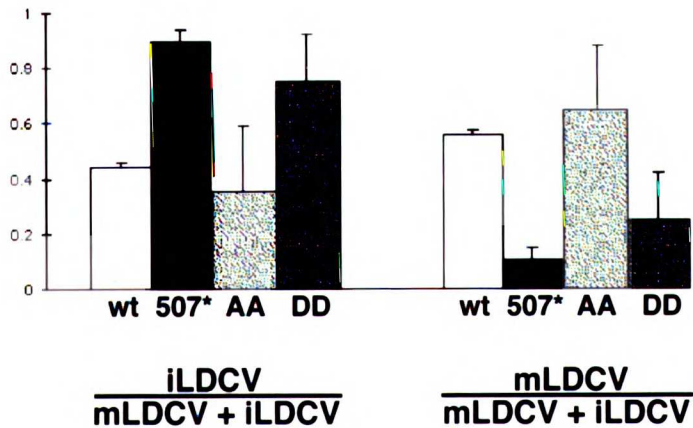
A**mature LDCV****B****immature LDCV****C**

Figure 6. AA and DD VMAT2 differ in the extent of colocalization with SgII

PC12 cells stably expressing AA or DD VMAT2 were double stained for HA using secondary antibodies conjugated to Cy3 (a, d) and for SgII using secondary antibodies conjugated to Cy5 (b, e). The cells were then examined by confocal microscopy. The merged Cy3 and Cy5 images are shown in c and f. The AA mutant colocalizes strongly with SgII, primarily at the tips of cell processes. The DD mutant colocalizes with SgII in the tips of processes but also exhibits strong perinuclear staining (arrowheads). Bar, 10 μm .

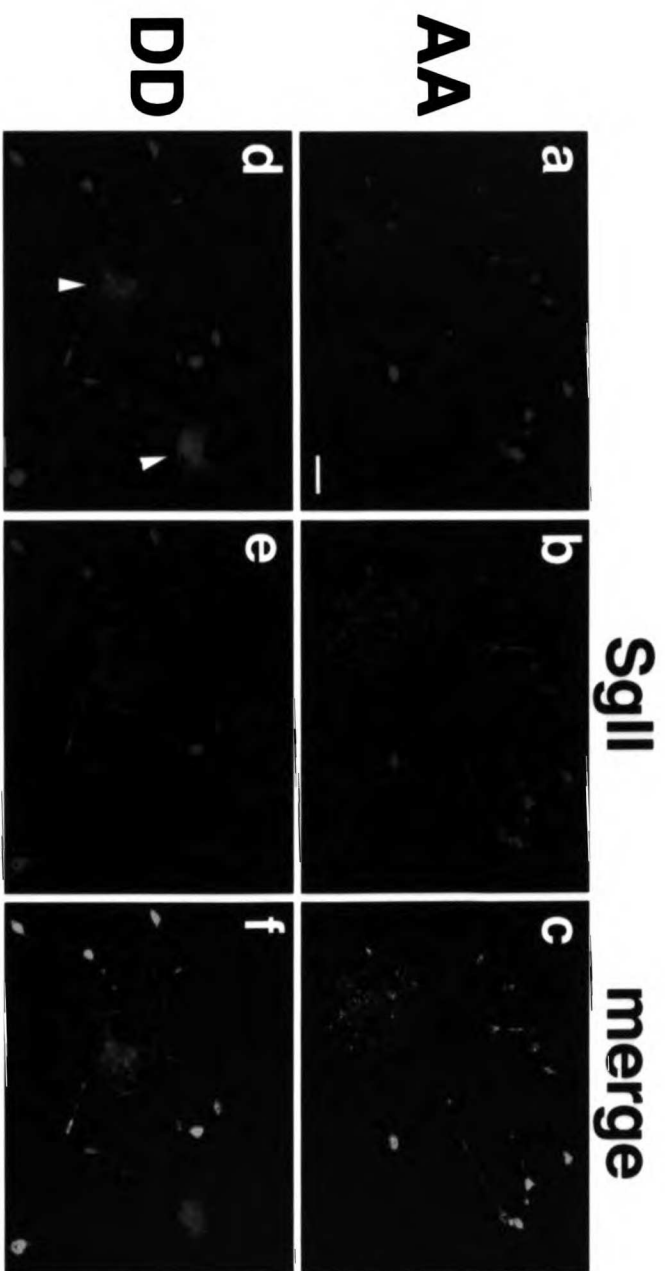


Figure 7. Density gradient fractionation of AA and DD VMAT2

Post-nuclear supernatants from PC12 cells stably expressing HA-tagged wild type (A), AA (B) and DD (C) VMAT2 were separated by equilibrium gradient centrifugation through 0.6-1.6 M sucrose and the fractions analyzed by Western blotting for HA (upper panels in A, B, and C), and SgII (lower panels). The gradients shown were then quantified using NIH Image and the amount of VMAT2 and SgII expressed as a fraction of the total immunoreactivity. Wild type and AA VMAT2 cofractionate with SgII in heavy fractions. DD also cofractionates with SgII but has a second peak in lighter fractions. The analysis of three different stable cell lines for each construct yielded similar results.

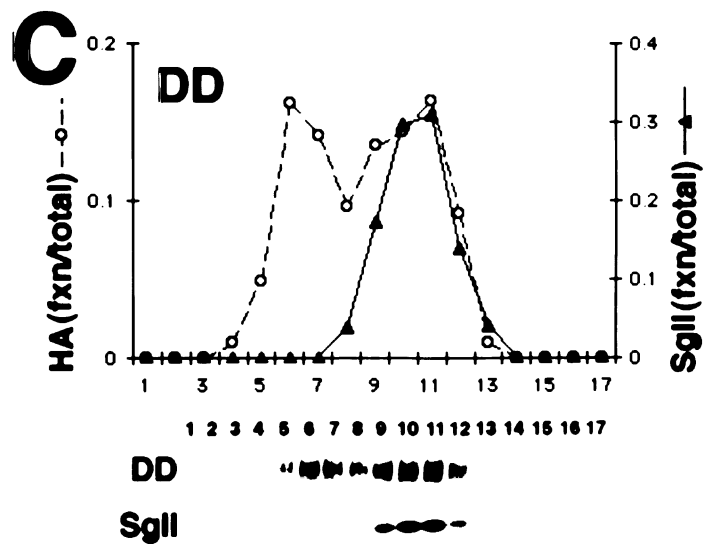
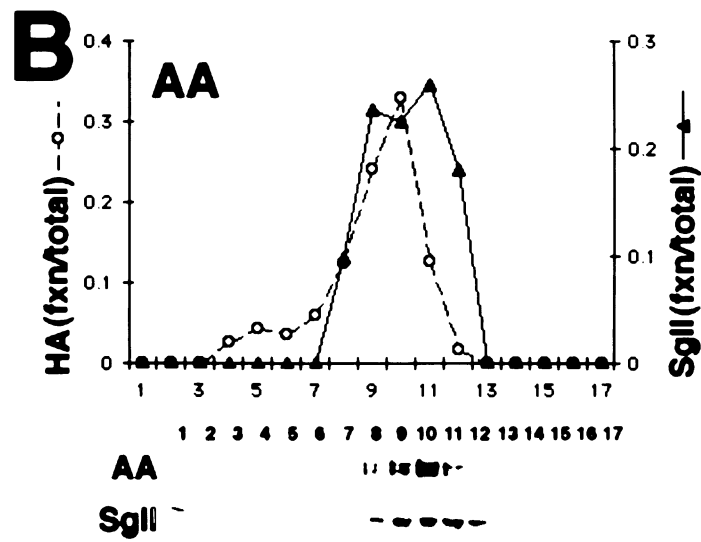
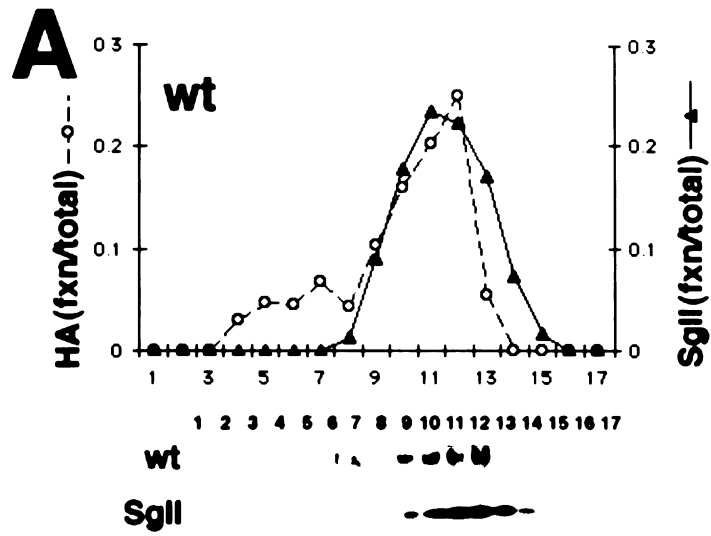


Figure 8. PACS-1 binding to the VMAT2 C-terminus

(A) GST fusion proteins containing the C-terminus of wild type VMAT2 or furin were bound to glutathione-Sepharose beads and phosphorylated using casein kinase 2.

Unphosphorylated and phosphorylated fusion proteins bound to glutathione-Sepharose were then incubated with a poly-His-tagged version of the PACS-1 furin-binding domain and the bound protein detected using an anti-polyhistidine antibody (PACS-1).

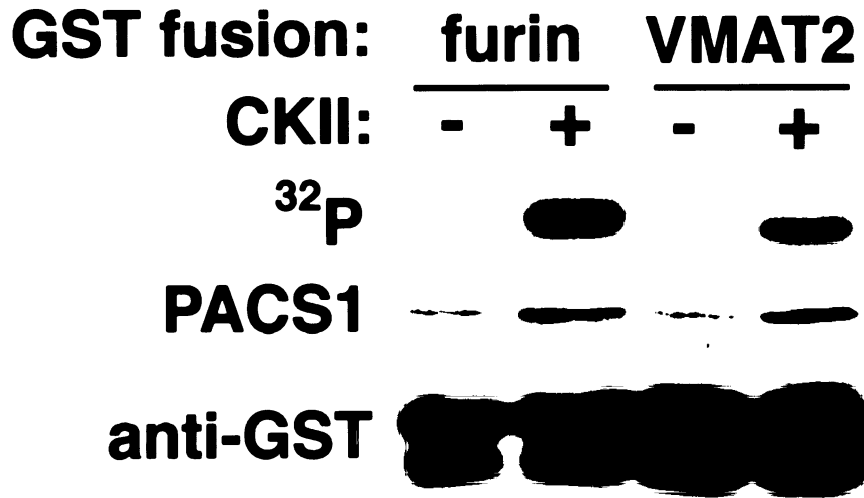
Autoradiography was used to assess protein phosphorylation (^{32}P). Western analysis for GST confirmed the presence of equal amounts of unphosphorylated and phosphorylated GST fusion proteins. Similar to phosphorylated furin, phosphorylated VMAT2 binds PACS-1 more strongly than the unphosphorylated protein.

(B) GST fusion proteins containing the C-termini of wild type, AA, DD, or 507*

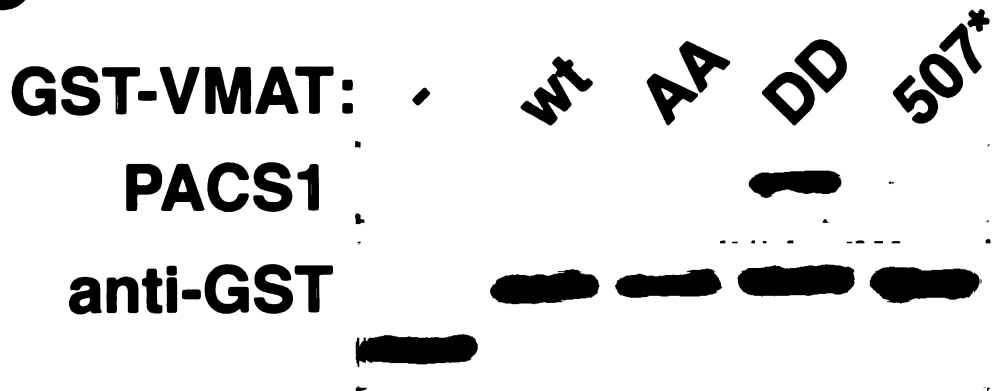
VMAT2 were incubated with the furin-binding domain of PACS-1 as described in A.

Western analysis was then used as described above to detect bound PACS-1 and confirm the presence of equal amounts of GST fusions. PACS-1 binds strongly to the DD mutant, but poorly to wild type VMAT2 and the AA mutant.

A



B



CHAPTER 3

A Dileucine-like Motif Targets Vesicular Monoamine Transporter 2 to the Regulated Secretory Pathway

Abstract

Large dense core vesicles (LDCVs) store and release a wide range of signaling molecules, from neural peptides to classical neurotransmitters, but little is known about their formation. Although proteins have been suggested to sort to LDCVs by aggregation of their luminal domains or association with lipid rafts, we have now identified a specific LDCV targeting signal in the cytoplasmic domain of the vesicular monoamine transporter 2 (VMAT2). VMAT2 contains a dileucine-like (isoleucine-leucine) motif and two glutamates 4 and 5 residues upstream. Replacement of either the dileucine-like motif or the upstream glutamates with alanine (IL/AA or EE/AA) reduces VMAT2 expression on LDCVs. We now show that both IL/AA and EE/AA mutants sort to the constitutive rather than the regulated secretory pathway. Since the IL motif is also required for endocytosis, the IL/AA mutant accumulates on the plasma membrane. However, the glutamates are not required for endocytosis and appear to have a specific role in sorting to LDCVs. Since EE/AA exhibits constitutive delivery to the plasma membrane and no defect in endocytosis, this mutant accumulates on synaptic-like microvesicles in PC12 cells. This work identifies one of the first signals that controls sorting to LDCVs, and is the first example of a dileucine motif involved in targeting to LDCVs.

Introduction

Neurons contain at least two distinct populations of secretory vesicles that undergo regulated exocytosis. Synaptic vesicles (SVs) store classical neurotransmitters and appear almost exclusively in nerve terminals, where they cluster at the synaptic cleft (Calakos and Scheller, 1996). In contrast, large dense core vesicles (LDCVs) store neuromodulatory peptides, growth factors and monoamines, and appear in cell bodies and dendrites as well as nerve terminals. SVs and LDCVs also differ in their modes of release. SVs mediate the rapid release of neurotransmitter into the synaptic cleft following an action potential, whereas LDCVs release their contents more slowly and in response to different stimuli, consistent with the neuromodulatory role of their contents (Kelly, 1993; Martin, 1994).

In addition to differences in content, subcellular localization and mode of release, LDCVs and SVs differ in biogenesis (Bauerfeind and Huttner, 1993; Kelly, 1993; Martin, 1994). LDCVs confer the regulated secretory pathway observed in neurons and other secretory cells, and bud directly from the trans-Golgi network (TGN) (Farquhar et al., 1978; Orci et al., 1987; Tooze and Tooze, 1986). After their formation, LDCVs undergo a maturation process in which membrane proteins destined for other intracellular compartments such as the TGN and lysosomes are removed (Klumperman et al., 1998; Tooze et al., 1991). In contrast, SVs do not bud from the TGN, but rather form near their site of release. Proteins destined for SVs sort into a constitutive secretory pathway at the

TGN, are continuously delivered to the plasma membrane in small cargo vesicles, and enter SVs after endocytosis (Cameron et al., 1991; Clift-O'Grady et al., 1990; Regnier-Vigouroux et al., 1991). Differences in protein targeting to LDCVs and SVs presumably underlie their differences in composition and function. However, relatively little is known about the signals that target proteins to LDCVs and SVs. To identify such signals, we have focused on a family of membrane proteins required for the packaging of neurotransmitter into vesicles.

Classical neurotransmitters are synthesized in the cytoplasm and require packaging into secretory vesicles for exocytotic release. Since specific transport proteins package these transmitters into secretory vesicles, the localization of these proteins to SVs or LDCVs determines the site of neurotransmitter storage and hence the mode of release. One family of transporter proteins includes two vesicular monoamine transporters (VMATs), VMAT1, expressed in peripheral, nonneural tissues, and VMAT2, expressed by monoamine neurons in the brain (Liu and Edwards, 1997b; Varoqui and Erickson, 1997). Consistent with the observed release of monoamines from cell bodies, dendrites, and nerve terminals in the brain, VMAT2 occurs on multiple populations of secretory vesicles. The protein localizes preferentially to LDCVs, but also appears on SVs and on tubulovesicular structures in the cell bodies and dendrites of dopamine neurons (Nirenberg et al., 1996; Nirenberg et al., 1997; Nirenberg et al., 1995). Since the localization of VMAT2 determines the site and mode of monoamine release, the targeting

of VMAT2 to LDCVs and other secretory vesicles presumably has important implications for signaling by monoamines.

As an integral membrane protein, VMAT2 contains cytoplasmic signals that direct its trafficking to LDCVs. In previous work, we have used heterologous expression in PC12 cells to identify one such signal. We showed that a cluster of acidic residues at the distal cytoplasmic C-terminus (DDEESESD), including two serines phosphorylated by casein kinase 2, is required for VMAT2 retention on LDCVs (Waites et al., 2001). Deletion of this motif or replacement of the serines with aspartate to mimic phosphorylation promotes VMAT2 removal from LDCVs during their maturation. The acidic cluster thus appears to retain VMAT2 on LDCVs.

In previous work, we have also identified a dileucine-like motif in the cytoplasmic C-terminus of VMAT2. An isoleucine-leucine pair (IL) within the sequence KEEKMAIL promotes the internalization of VMAT2 from the plasma membrane. Replacement of IL by alanine (IL/AA) reduces VMAT2 maturation by >50% (Tan et al., 1998). In other proteins, acidic residues 4 and 5 positions upstream of the dileucine signal are also required for endocytosis (Dietrich et al., 1997; Pond et al., 1995), and VMAT2 contains highly conserved glutamates at these positions. However, replacement of glutamates 478 and 479 with alanine does not impair VMAT2 endocytosis (Tan et al., 1998). Since dileucine motifs are known to mediate trafficking at multiple sites in the cell, we considered that these residues may influence other sorting events. Indeed, the

closely-related vesicular acetylcholine transporter (VACHT) also contains a dileucine motif, and we have shown that the residues 4 and 5 positions upstream of the leucines (Ser-480 and Glu-481) influence sorting to LDCVs (Krantz et al., 2000). In VACHT, S480 undergoes regulated phosphorylation by an isoform of protein kinase C (Krantz et al., 2000). Replacement of S480 by glutamate to mimic phosphorylation increases the localization of VACHT to LDCVs, while replacement with alanine to prevent phosphorylation decreases localization of VACHT to LDCVs (Krantz et al., 2000). Thus, negative charge 5 residues upstream of a dileucine motif increases the targeting of VACHT to LDCVs. Since VMAT2 sorts primarily to LDCVs and has acidic residues at both -4 and -5 relative to the IL signal, it seems likely that these residues also promote the targeting of VMAT2 to LDCVs.

We now find that Glu-478 and -479 mediate the targeting of VMAT2 to LDCVs. Replacement of these residues by alanine (EE/AA) decreases the localization of VMAT2 to LDCVs and increases its localization to SLMVs. In addition, we show that both the glutamates and the IL signal are required for sorting into LDCVs at the TGN. This data provides the first example of a motif involved in targeting to nascent LDCVs.

Materials and Methods

Mutagenesis, Cell Culture, and Immunofluorescence. Mutagenesis was performed using the Kunkel method (Kunkel et al., 1991) as previously described (Tan et al., 1998). PC12 cell transfection, isolation of independent cell clones, and immunofluorescence were done as previously described (Krantz et al., 2000; Liu and Edwards, 1997a). For the HA antibody internalization experiments, cells were first plated onto poly-L-lysine and Matrigel (Becton Dickinson)-coated coverslips and treated with NGF for 2-3 days. Cells were next incubated with HA.11 mouse monoclonal antibody (Covance) diluted 1:100 in standard PC12 medium for 1 hour at 37°C, then washed three times in medium before fixation and staining. Immunostained cells were visualized by confocal laser microscopy.

Cell Fractionation. PC12 cell membranes were prepared as previously described (Liu and Edwards, 1997a). Briefly, cells were harvested into Buffer A (150 mM NaCl, 10 mM Hepes, pH 7.4, 1 mM EGTA, 0.1 mM MgCl₂) and protease inhibitors, then homogenized at 10 μ M clearance. Nuclei and debris were pelleted at 1000g for 8 minutes and the resulting post-nuclear supernatant (PNS) was loaded onto the appropriate gradient for fractionation.

For equilibrium sedimentation, PNS was layered onto a linear 0.6-1.6M sucrose gradient and sedimented to equilibrium at 30,000 rpm for 12-16 hours in an SW41 rotor at 4°C. Fractions were collected from the top of the tube.

For velocity sedimentation, PNS was loaded onto a 5-25% glycerol gradient containing Hepes-buffered saline (0.15M NaCl, 25 mM Hepes, pH 7.2) and centrifuged at 37,000 rpm in an SW41 rotor for 1 hr at 4°C. Fractions were collected from the top.

Western analysis and quantitation. Proteins were separated by electrophoresis through SDS-polyacrylamide, electroblotted to nitrocellulose, and immunostained as previously described (Krantz et al., 2000). After detection of bound antibodies using SuperSignal West Pico (Pierce), films were optically scanned, digitized, and quantified using NIH Image. For sucrose equilibrium and glycerol velocity gradients, the amount of HA, SgII, or synaptophysin immunoreactivity in each gradient fraction was expressed as a fraction of the total HA, SgII, or synaptophysin in all gradient fractions.

Pulse-chase analysis. Metabolic labeling with ³⁵S-cysteine/methionine was performed according to standard procedures. PC12 cells were rinsed twice with cysteine/methionine free medium (Gibco), incubated at 37°C for 30 minutes, then labeled for 30 minutes in the same medium containing 0.5 mCi/ml ³⁵S-cysteine/methionine (Expre³⁵S³⁵S Protein Labeling mix, NEN). Cells were next washed once in standard PC12 medium containing

cysteine and methionine, then incubated at 37°C in this medium for 1, 2, or 3 hours. To detect ³⁵S-labeled VMAT2 on the plasma membrane at each timepoint, HA.11 antibody (1:100 dilution) was added to the medium of half the cells during their last hour of incubation. The remaining cells were used to measure total ³⁵S-labeled VMAT2 at each timepoint. After the final incubation, cells were washed three times in ice-cold PBS and harvested into immunoprecipitation (IP) buffer (50 mM Tris, pH 7.5, 150 mM NaCl, 10 mM EDTA, 5 mM EGTA, 1% Triton X-100, 0.2% SDS, 20 µg/ml PMSF, 2 µg/ml pepstatin, 2 µg/ml leupeptin). Following a 10 minute incubation on ice to solubilize proteins, debris was pelleted at 16,000 g for 10 minutes and the resulting supernatant subject to immunoprecipitation. To detect cell-surface VMAT2 at each timepoint, supernatants from cells exposed to HA.11 antibody during the final incubation were incubated with protein G-coated agarose beads (Amersham-Pharmacia). To detect total VMAT2 at each timepoint, remaining supernatants were incubated with protein G beads conjugated to HA.11 antibody. Following overnight incubation at 4°C, protein G beads were spun down and washed three times with ice-cold IP buffer. Proteins were eluted from the beads with 3X SDS sample buffer (New England Biotech) and subject to SDS-PAGE.

Autoradiography and quantitation. Following SDS-PAGE, gels were fixed in 50% methanol, 10% acetic acid for 30 minutes, washed multiple times in deionized water, then

incubated in 1 M salicylate for 30 minutes. Gels were then dried onto filter paper and exposed to film (Biomax MS, Kodak) at -70°C using an intensifying screen (Transcreen LE, Kodak). Developed films were optically scanned, digitized, and quantified using NIH Image.

To quantify the pulse-chase experiments, amounts of ^{35}S -labeled VMAT2 detected on the cell-surface at 1, 2, and 3 hours were expressed as fractions of the total ^{35}S -labeled VMAT2 present at these timepoints. Pulse-chase analysis was conducted three times for each VMAT2 protein studied (wild-type, IL/AA, and EE/AA).

Results

We have previously shown that an IL signal mediates the internalization of VMAT2 from the plasma membrane, but glutamates 4 and 5 residues upstream of this motif do not affect internalization (Tan et al., 1998). To determine whether these acidic residues mediate other aspects of VMAT2 trafficking, we analyzed the steady-state localization of the E478A/E479A (EE/AA) mutant in PC12 cells. Immunofluorescence of stably transfected cells shows that wild-type VMAT2 colocalizes precisely with the LDCV marker secretogranin II (SgII) at the tips of processes (Fig. 1, a-c). Both proteins are virtually absent from cell bodies. The EE/AA mutant also colocalizes with SgII at the tips of processes, but in addition shows strong staining in cell bodies (Fig. 1, d-f). Another protein that exhibits strong staining in both cell bodies and tips of processes is the SLMV marker synaptophysin (syn) (Fig. 1, h and k). Indeed, in contrast to wild-type VMAT2 (Fig. 1, g-i), EE/AA colocalizes strongly with synaptophysin (Fig. 1, j-l). Thus, glutamates upstream of the IL signal appear to have a role in the trafficking of VMAT2, perhaps by directing the protein into SLMVs.

To further assess how the EE/AA mutation alters the localization of VMAT2, we used equilibrium sedimentation through sucrose, which separates LDCVs from SLMVs. As previously observed, wild-type VMAT2 cofractionates predominantly with SgII in heavy, LDCV-containing fractions and only to a minor degree with synaptophysin in lighter SLMV-containing fractions (Fig. 2A) (Krantz et al., 2000). In contrast, EE/AA

cofractionates less well with SgII and to a greater extent with synaptophysin (Fig. 2, B and C). This analysis suggests that neutralization of Glu-478 and -479 redistributes VMAT2 out of LDCVs and into SLMVs.

To confirm that the EE/AA mutant observed in light fractions of the sucrose density gradient is associated with SLMVs rather than contaminating membranes, we analyzed the mutant by velocity gradient fractionation. Velocity sedimentation through glycerol separates SLMVs from most other membranes (Clift-O'Grady et al., 1990). SLMV-containing fractions 5-8 contain synaptophysin (Fig. 3, lower panels). Wild-type VMAT2, which is present at very low levels on SLMVs, is undetectable in these fractions and appears only at the bottom of the gradient (Fig. 3A). In contrast, EE/AA cofractionates with synaptophysin in peak SLMV fractions (Fig. 3B). Indeed, almost 40% of the total EE/AA protein can be detected in fractions 6-7, indicating that EE/AA does appear on SLMVs.

Since wild-type VMAT2 appears almost exclusively on LDCVs, how does EE/AA enter SLMVs? Most synaptic vesicle proteins enter SLMVs after internalization from the plasma membrane, where they are initially delivered via the constitutive secretory pathway (Bauerfeind and Huttner, 1993; Kelly, 1991). In contrast, VMAT2 sorts to LDCVs, which comprise the regulated secretory pathway. However, neutralization of Glu-478 and -479 may redirect VMAT2 into the constitutive pathway, thus delivering the protein to the plasma membrane and allowing it to enter SLMVs. We

have already observed that replacement of the IL motif with alanine (IL/AA) mislocalizes VMAT2 to the plasma membrane (Tan et al., 1998), and this mutation may interfere with sorting in the TGN as well as endocytosis. In contrast, the EE/AA mutant exhibits normal internalization from the plasma membrane but may enter SLMVs through the constitutive secretory pathway.

If IL/AA and EE/AA do enter the constitutive rather than the regulated secretory pathway, we should detect higher levels of these mutants at the plasma membrane. To assess VMAT2 delivery to the plasma membrane, we used an antibody internalization assay. All the VMAT2 constructs we have used contain a luminal HA epitope tag that can bind HA antibody in the culture medium when VMAT2 resides on the plasma membrane. Monoclonal HA.11 antibody was added to the medium of cells stably expressing wild-type VMAT2, EE/AA, IL/AA and two other mutations in the KEEKMAIL motif, K477A (K/A) and K480A/M481A (KM/AA). The K/A and KM/AA mutants do not appear to alter the steady-state localization of VMAT2 (data not shown), but we nevertheless wanted to directly compare the role of all residues in the motif. Cells were incubated for 1 hour at 37°C to allow antibody binding and internalization, then fixed and examined by immunofluorescence using a secondary anti-mouse antibody and a rat HA antibody to assess total VMAT2 expression. We observed very little antibody internalization by wild-type VMAT2, despite high levels of VMAT2 expression (Fig. 4, a-b). Similarly, K/A and KM/AA mutants exhibit low levels of

antibody uptake, indicating that very little of these proteins are delivered to the plasma membrane (Fig. 4, c-d, g-h). In contrast, EE/AA and IL/AA exhibit high levels of antibody uptake, approximating the total amount of VMAT2 in these cells (Fig. 4, e-f, i-j). These results indicate that large amounts of EE/AA and IL/AA are delivered to the plasma membrane.

The increased plasma membrane delivery of EE/AA and IL/AA mutants relative to wild-type VMAT2 could reflect differences in sorting to the regulated secretory pathway. Alternatively, wild-type and mutant proteins may both cycle repeatedly between the plasma membrane and TGN before sorting to LDCVs, with inefficient recycling of the mutants contributing to increased plasma membrane delivery. To distinguish between these possibilities, we used a metabolic labeling procedure to determine how rapidly EE/AA and IL/AA appear on the plasma membrane after biosynthesis. If the newly-synthesized proteins are detected at the cell surface within a short period of time, this would indicate sorting to the constitutive secretory pathway. Proteins in the regulated pathway presumably do not reach the plasma membrane until stimulation of LDCV exocytosis. Stably transfected cells were labeled for 30 minutes with ³⁵S-cysteine/methionine, then incubated in medium containing unlabeled cysteine/methionine for 1, 2, or 3 hours. During the last hour of incubation, HA.11 antibody was added to the medium of half the cells to detect labeled VMAT2 at the plasma membrane. Total or cell-surface ³⁵S-labeled VMAT2 was then

immunoprecipitated from cell extracts and subject to autoradiography. As anticipated, wild-type VMAT2 is virtually undetectable at the cell surface for all timepoints despite high levels of total protein expression (Fig. 5A). In contrast, large amounts of EE/AA and IL/AA appear at the cell surface even at the earliest timepoints (Fig. 5A). The mutants can be detected at the plasma membrane within an hour of synthesis in the ER, suggesting that they are sorted into the constitutive secretory pathway.

To quantify these results, the metabolic labeling/immunoprecipitation procedure was repeated three times for each VMAT2 construct and densitometry was used to measure amounts of total and cell-surface protein for each timepoint. For all VMAT2 constructs, the amount of cell-surface protein was expressed as a fraction of total protein, and average fractions were calculated for each timepoint. This analysis definitively demonstrates that very little wild-type VMAT2 is delivered to the plasma membrane (less than 20% of the total labeled protein for any timepoint), while large proportions of EE/AA and IL/AA are (Fig. 5B). About 80% of total labeled IL/AA and 60% of EE/AA appear on the cell surface within an hour of synthesis, indicating that these mutant VMATs are redirected from the regulated to the constitutive secretory pathway (Fig. 5B). Thus, glutamates 478 and 479 and the IL signal are necessary for targeting VMAT2 to the regulated secretory pathway.

If the IL motif and upstream glutamates direct VMAT2 into the regulated secretory pathway, what is their relationship to the previously-identified acidic cluster

motif which retains VMAT2 on LDCVs? We expect protein sorting into the regulated secretory pathway to occur prior to retention on LDCVs. Thus, the IL signal and upstream glutamates should influence VMAT2 trafficking before the acidic cluster. To test this hypothesis, we made a VMAT2 construct containing both the 507* deletion of the acidic cluster and the IL/AA mutation (IL507*). If the IL signal affects VMAT2 trafficking first, IL507* should resemble IL/AA and appear on the plasma membrane. Indeed, when IL507* was stably expressed in PC12 cells and analyzed by immunofluorescence, we found it to have the same phenotype as IL/AA (Fig. 6, g-l). In contrast to wild-type VMAT2, which colocalizes with SgII at tips of processes (Fig. 6, a-c), and 507*, which appears in a perinuclear region (Fig. 6, d-f), IL/AA and IL507* both appear at high levels on the plasma membrane (Fig. 6, g-l). These results demonstrate that the dileucine-like motif acts upstream of the acidic cluster in VMAT2 trafficking, presumably in the trans-Golgi network.

Discussion

This study demonstrates that a dileucine-like signal and glutamates 4 and 5 positions upstream target VMAT2 to LDCVs. We have previously shown that replacement of the IL signal with alanine (IL/AA) significantly impairs VMAT2 endocytosis and mislocalizes VMAT2 to the plasma membrane. In contrast, replacement of the upstream glutamates with alanine (EE/AA) does not affect internalization (Tan et al., 1998). We now show that the EE/AA mutation does alter VMAT2 steady-state localization by redistributing the protein from LDCVs to SLMVs. In addition, both IL/AA and EE/AA redirect VMAT2 from the regulated to the constitutive secretory pathway and cause high levels of protein delivery to the plasma membrane. Since IL/AA is defective in endocytosis, this mutant accumulates on the plasma membrane, whereas EE/AA undergoes endocytosis and apparently sorts to SLMVs. Other residues in the KEEKMAIL motif do not appear to affect the targeting of VMAT2 to LDCVs, indicating that the IL signal and glutamates 478 and 479 may be sufficient to mediate this trafficking event. This data provides the first example of a specific LDCV targeting motif, which appears to be a dileucine motif.

Very few if any signals that target integral membrane proteins to LDCVs have been identified. The domain responsible for targeting the enzyme peptidylglycine α -amidating monooxygenase (PAM) to LDCVs has been identified, but this domain is luminal rather than cytoplasmic (Milgram et al., 1996). Thus, the targeting of PAM to

LDCVs is presumably dependent upon interactions with soluble LDCV contents, which sort into nascent LDCVs as a result of pH and redox-dependent aggregation. In contrast, most integral membrane proteins are thought to enter LDCVs by interacting with cellular sorting machinery through cytoplasmic targeting signals. The endothelial protein P-selectin also sorts partially to LDCVs when expressed in PC12 cells, and appears to be targeted to these vesicles by the cytoplasmic tyrosine-based motif YGVF (Blagoveshchenskaya et al., 1999). However, this sequence is also responsible for targeting P-selectin to SLMVs (Blagoveshchenskaya et al., 1999), suggesting that it is not specific for LDCV targeting. Indeed, most of the integral membrane proteins present on LDCVs are also present on SLMVs, including the vSNARE proteins involved in vesicle docking and fusion (Glenn and Burgoyne, 1996; Schmidle et al., 1991) and certain isoforms of the calcium sensor synaptotagmin (Schmidle et al., 1991; Walch-Solimena et al., 1993). Thus, identifying signals that specifically target proteins to the regulated secretory pathway has been difficult. Because VMAT2 sorts almost exclusively to LDCVs, such an analysis has been possible, and we have found a sequence that specifically targets VMAT2 to the regulated secretory pathway.

Dileucine-based signals are one of the most common integral membrane protein sorting motifs. These motifs typically contain at least one leucine and a second hydrophobic residue such as leucine, isoleucine, methionine, or valine (Sandoval and Bakke, 1994). Certain proteins also contain acidic residues 4 and 5 positions upstream of

the dileucine signal which can influence its role in trafficking. Dileucine motifs mediate a variety of protein sorting events, including endocytosis, lysosomal and endosomal targeting, and basolateral targeting in polarized cells (Hunziker and Fumey, 1994; Kirchhausen et al., 1997; Sandoval and Bakke, 1994). Recently, they have also been shown to direct certain proteins to SLMVs in PC12 cells (Blagoveshchenskaya et al., 1999). However, this paper provides the first example of a dileucine-based motif involved in targeting to the regulated secretory pathway.

The dileucine-like motif in VMAT2 appears to mediate both endocytosis and targeting to LDCVs. Since dileucine signals mediate sorting at multiple sites within the cell, even for a single protein, how is the same signal recognized at different sites? Clathrin adaptor protein (AP) complexes, which have distinct subcellular localizations and regulate different sorting events, may account for selective recognition. Dileucine motifs have been shown to bind both AP-1, which is found at the TGN and mediates endosomal/lysosomal sorting, and AP-2, the adaptor complex that facilitates clathrin-mediated endocytosis at the plasma membrane (Heilker et al., 1996; Kirchhausen et al., 1997). Recent evidence also indicates that they interact with AP-3, an adaptor involved in lysosomal sorting and SLMV budding from endosomes (Faundez et al., 1998; Honing et al., 1998; Odorizzi et al., 1998). Thus, the IL signal in VMAT2 could mediate endocytosis by interacting with AP-2 at the plasma membrane, and targeting to LDCVs by interacting with AP-1 or another adaptor complex in the TGN.

Specificity for the dileucine-like motif in VMAT2 could also be conferred by the glutamates 4 and 5 positions upstream. We have shown that these residues do not affect VMAT2 endocytosis, but do influence targeting to LDCVs. The EE/AA mutation decreases the targeting of VMAT2 to LDCVs and substantially increases targeting to the constitutive secretory pathway, allowing VMAT2 to enter SLMVs. Likewise, equivalent residues in the closely related VACHT influence sorting to LDCVs (Krantz et al., 2000). We propose that the acidic residues influence VMAT2 and VACHT targeting to LDCVs by stabilizing interactions between their dileucine signals and a TGN-based adaptor complex required for LDCV targeting. When these acidic residues are neutralized, the adaptor complex does not bind as effectively to the dileucine motifs, and targeting to LDCVs is reduced. This hypothesis is supported by several pieces of data. We observe a decrease in targeting to LDCVs when the acidic residues in VMAT2 or VACHT are replaced by alanine, and an increase in VACHT targeting to LDCVs when the serine in VACHT is replaced by a more acidic glutamate (Krantz et al., 2000). In addition, proportionately less of the EE/AA mutant is targeted to the constitutive secretory pathway than of the IL/AA mutant, suggesting that replacement of the acidic residues with alanine has less of an effect on this sorting event than replacement of the IL signal. Thus, it seems likely that the IL signal is the primary targeting sequence and that the upstream glutamates have a secondary role. Pulse-chase analysis also indicates that the

sorting event affected by these mutations occurs in the biosynthetic pathway, indicating that a TGN-associated adaptor complex might be involved.

Three AP complexes have been shown to associate with the TGN, and any of these could interact with the dileucine sequences on VMAT2 or VACHT. AP-1 has been shown to interact with dileucine motifs (Rapoport et al., 1998) and is found on small vesicles budding from the TGN (Klumperman et al., 1998). Patches of AP-1 have also been observed on LDCVs by electron microscopy, but they are thought to mediate the removal of excess membrane and proteins destined for other compartments rather than the budding of LDCVs (Klumperman et al., 1998). Nevertheless, AP-1 could play a role in LDCV biogenesis, and could target VMAT2 to LDCVs by binding to the dileucine-like motif. AP-3 has also been shown to interact with dileucine motifs and is implicated in both the biogenesis and cargo selection of pigment granules, melanosomes, and platelet dense granules (Kantheti, 1998; Ooi et al., 1997; Simpson et al., 1997).

Therefore, this adaptor might be expected to have a role in LDCV biogenesis and protein targeting. However, there is no evidence for such a role; instead, AP-3 has been shown to be involved in lysosomal targeting and SLMV formation (Faundez et al., 1998; Odorizzi et al., 1998). The recently identified adaptor AP-4 also associates with the TGN or an adjacent structure and its function is currently unknown (Dell'Angelica et al., 1998). Further studies are needed to determine whether this adaptor interacts with dileucine sequences, and whether it could be involved in LDCV biogenesis or protein targeting.

In addition to endocytosis and LDCV targeting, could other VMAT2 trafficking events be mediated by the dileucine-like motif? Antibody internalization studies indicate that when the IL/AA mutant does undergo endocytosis, it localizes to a different compartment than wild-type VMAT2 and the EE/AA mutant. Thus, the IL signal, but not the upstream glutamates, may also be required for targeting VMAT2 to a specific compartment after endocytosis. Preliminary evidence suggests that after the regulated exocytosis of LDCVs, some proportion of wild-type VMAT2 enters SLMVs following internalization from the plasma membrane (C. Waites, unpublished observations). An even greater proportion of EE/AA is found on SLMVs, presumably because so much of the mutant protein appears at the plasma membrane constitutively. Another study has shown that dileucine signals mediate the targeting of synaptotagmin and tyrosinase to SLMVs (Blagoveshchenskaya et al., 1999). Thus, the IL signal could play a role in targeting VMAT2 to SLMVs following endocytosis as well as in endocytosis itself. This sorting event would presumably occur after the regulated exocytosis of LDCVs, which is the only time that wild-type VMAT2 appears at the plasma membrane. However, additional experiments are needed to confirm this role for the IL signal.

We have previously shown that an acidic cluster motif influences the sorting of VMAT2 to LDCVs (Waites et al., 2001). However, this motif mediates the retention of VMAT2 on LDCVs during their maturation rather than entry into LDCVs at the TGN. We now show that an IL signal and upstream glutamates mediate this initial sorting

event, directing VMAT2 into the regulated secretory pathway. This motif is necessary for proper sorting of VMAT2 to LDCVs, and provides the first example of a specific LDCV targeting signal.

Figures

Figure 1. Neutralization of glutamates-478 and -479 in VMAT2

To neutralize the acidic residues upstream of the dileucine motif in VMAT2, Glu-478 and -479 were replaced by alanine. PC12 cells stably expressing wild-type VMAT2 and the E478A/E479A mutant (EE/AA) were double-stained with a mouse monoclonal antibody to the HA epitope (a, d, g, j) and either a rabbit polyclonal antiserum to SgII (b and e), or a rabbit antibody to synaptophysin (syn; h and k). Secondary anti-mouse antibodies conjugated to Cy3 (a, d, g, and j) or anti-rabbit antibodies conjugated to Cy5 (b, e, h, and k) were used to visualize the proteins, and the cells were examined by confocal microscopy. The merged Cy3 and Cy5 images are shown in c, f, i, and l. Wild-type VMAT2 colocalizes with both SgII and synaptophysin at the tips of processes, but does not colocalize with synaptophysin in cell bodies. In contrast, the EE/AA mutant is present at high levels in cell bodies and exhibits greater colocalization with synaptophysin than wild-type VMAT2. Bars, 10 μ m.

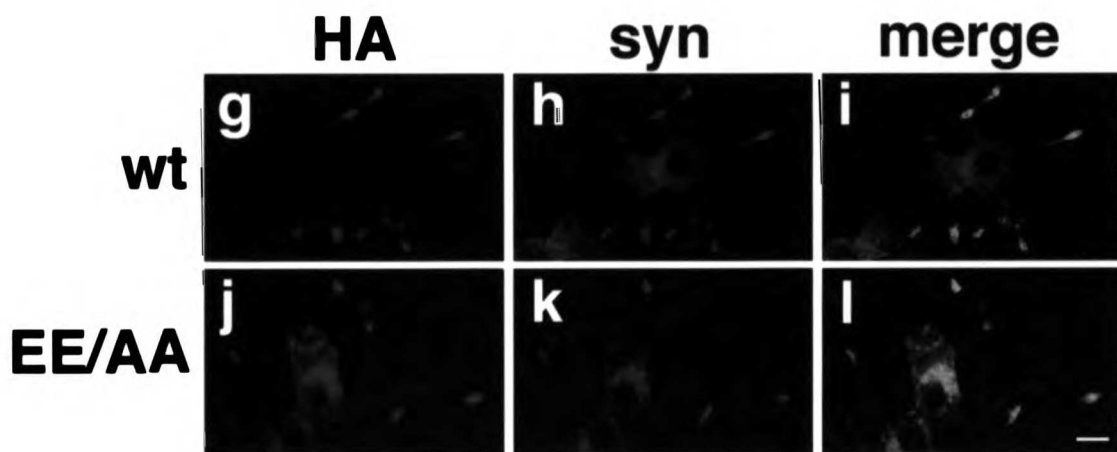
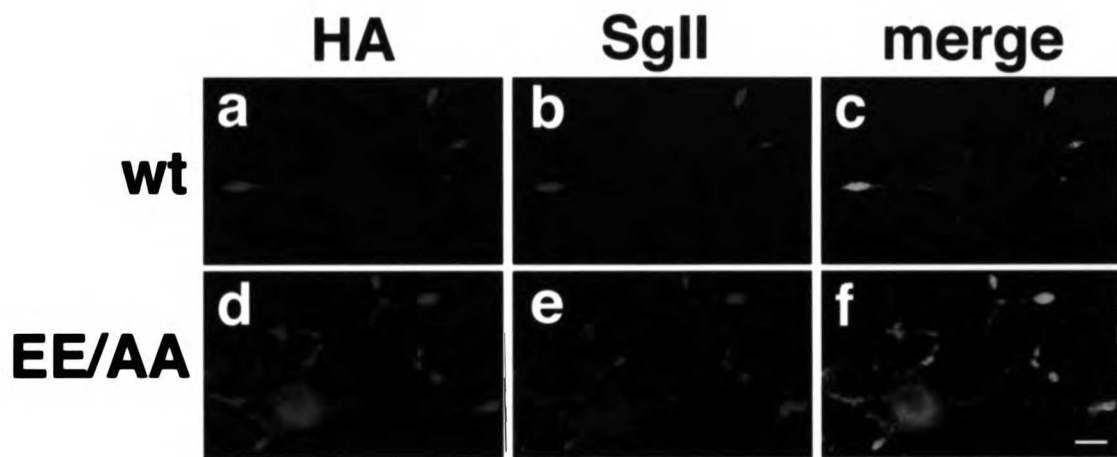


Figure 2. The E478A/E479A mutation redistributes VMAT2 away from LDCVs

Post-nuclear supernatants of PC12 cells stably expressing HA-tagged wild-type VMAT2

(A) and the EE/AA mutant (B) were separated by equilibrium sedimentation through 0.6-

1.6 M sucrose. The fractions were analyzed by Western blot using a monoclonal HA

antibody for VMAT2 (top of immunoblots in A and B), a polyclonal antibody to SgII

(middle), and a monoclonal antibody to synaptophysin (bottom). The immunoblots

shown in A and B were digitized, quantified, and the amounts of HA-tagged VMAT2,

synaptophysin, and SgII were expressed as a percentage of total immunoreactivity. Wild-

type VMAT2 cofractionates more strongly with SgII than with synaptophysin. In

contrast, the EE/AA mutation shifts VMAT2 into lighter membrane fractions.

(C) The proportion of VMAT2 localized to peak synaptophysin fractions (left) or peak

SgII fractions was expressed as a percentage of total VMAT2 immunoreactivity across

the gradients, using the data shown in A and B and two additional independently isolated

cell lines for each mutant. The bar graph shows the mean +/- standard error ($n=3$).

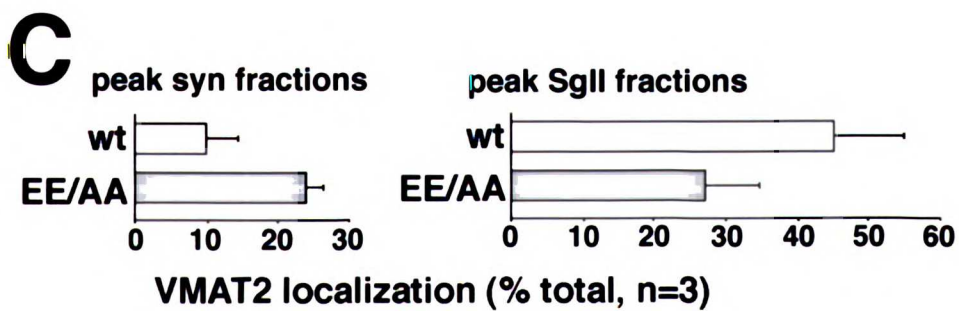
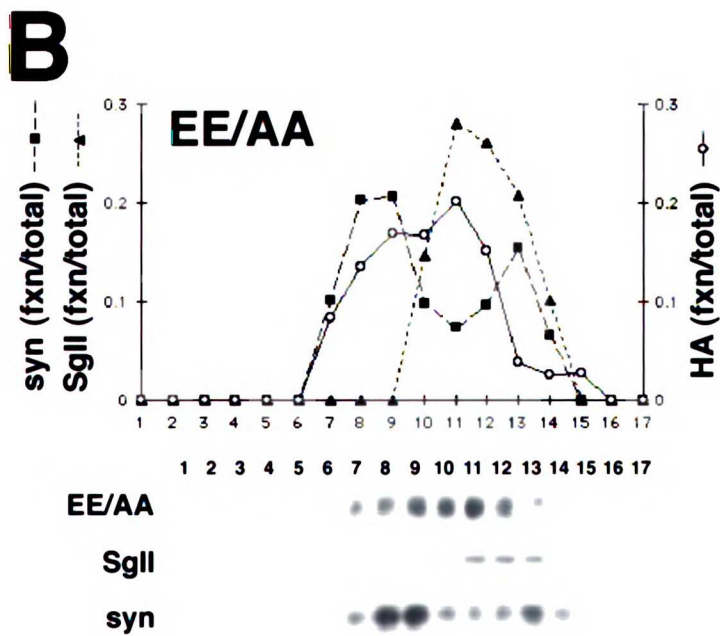
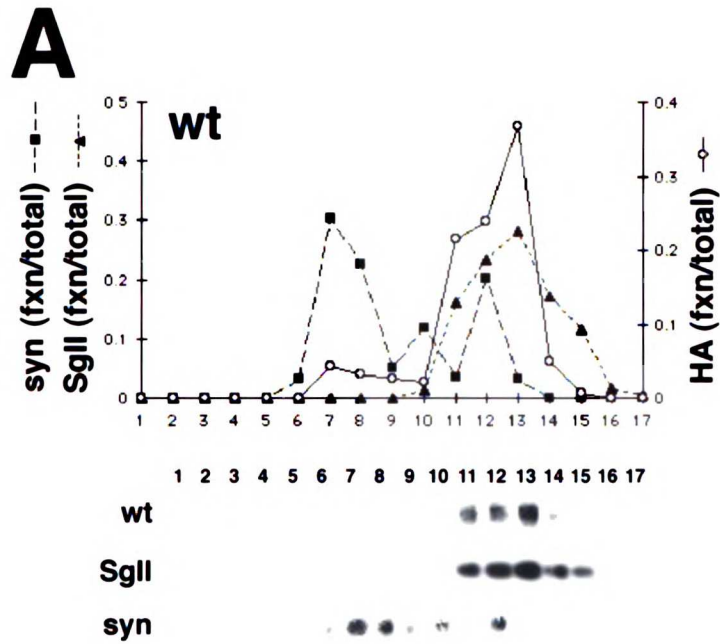


Figure 3. EE/AA cofractionates with synaptophysin in synaptic-like microvesicles

Post-nuclear supernatants from PC12 cells stably expressing HA-tagged wild type (A) and EE/AA (B) VMAT2 were separated by velocity gradient centrifugation through 5-25% glycerol. Fractions were collected and analyzed by Western blot using the monoclonal HA antibody to detect VMAT2 (upper panels in A and B) and a polyclonal antibody to detect the synaptic-like microvesicle (SLMV) marker synaptophysin (lower panels). The immunoblots were then digitized and quantified using NIH Image. For each fraction, the amount of VMAT2 and synaptophysin is expressed as a percentage of total immunoreactivity in all fractions. Wild type VMAT2 is undetectable in SLMV-containing fractions 5-7 and appears only at the bottom of the gradient. In contrast, almost 40% of the EE/AA protein cofractionates with synaptophysin in these fractions.

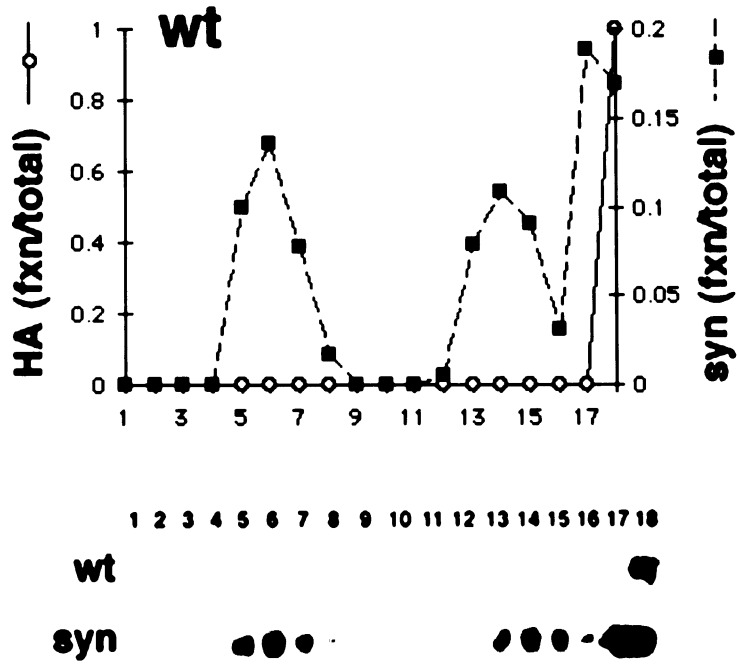
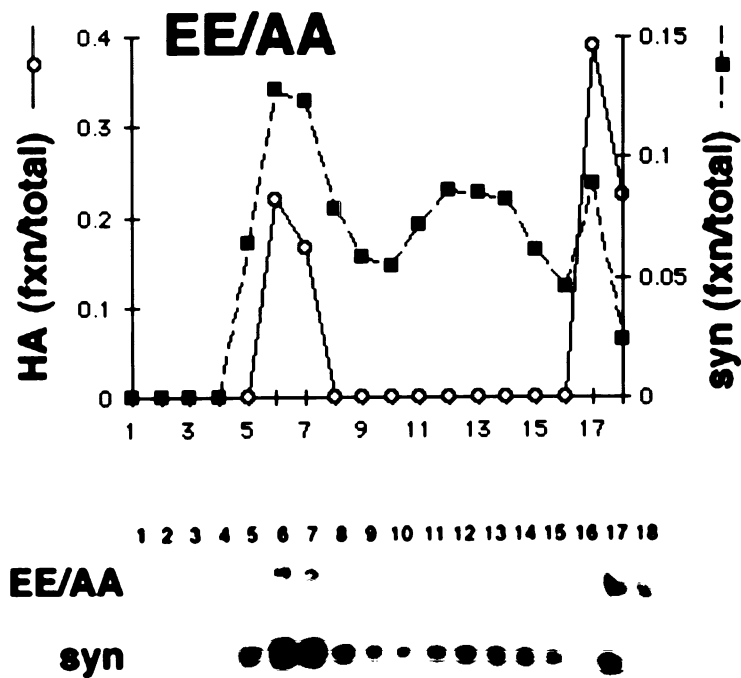
A**B**

Figure 4. The I483A/L484A and EE/AA mutations increase delivery of VMAT2 to the plasma membrane

PC12 cells stably expressing HA-tagged wild-type, K477A (K/A), EE/AA, K480A/M481A (KM/AA), or I483A/L484A (IL/AA) VMAT2 were incubated in medium containing HA.11 monoclonal antibody for 1 hour at 37°C. Cells were then fixed and stained with a rat monoclonal HA antibody followed by anti-mouse antibodies conjugated to FITC (a, c, e, g, i) and anti-rat antibodies conjugated to Texas Red (b, d, f, h, and j). Stained cells were examined by confocal microscopy. Confocal laser settings for each fluorophore were identical for all cells to accurately reflect protein levels. Cells expressing wild-type VMAT2 do not show significant HA antibody internalization (a) relative to total protein expression (b), suggesting low levels of VMAT2 delivery to the plasma membrane. Similarly, cells expressing K/A and KM/AA show only low levels of antibody internalization (c, g) despite high levels of VMAT2 expression (d, h). In contrast, cells expressing the EE/AA and IL/AA mutants exhibit high levels of antibody uptake (e, i), indicating that substantial amounts of these mutant VMATs are delivered to the plasma membrane.

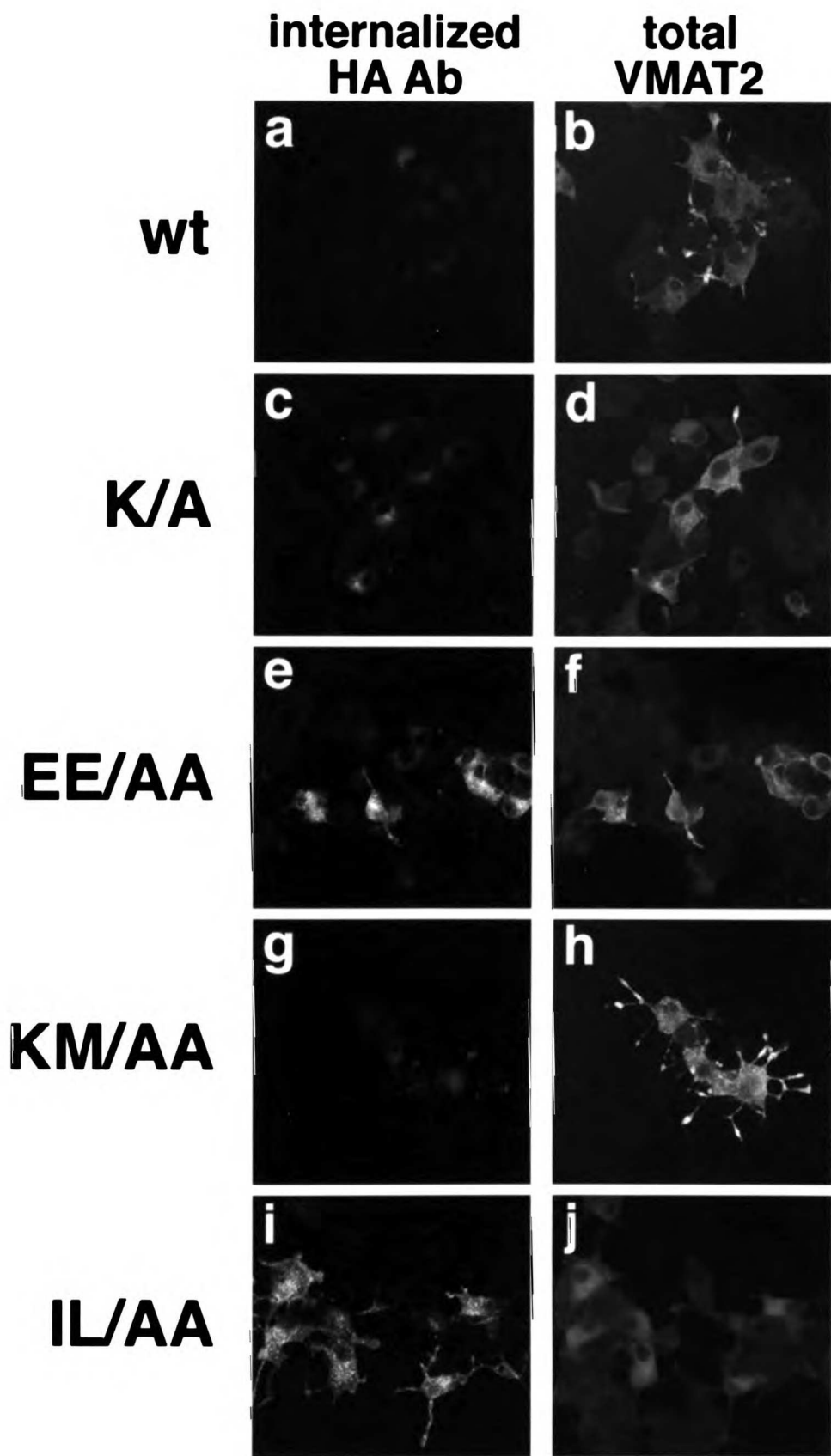
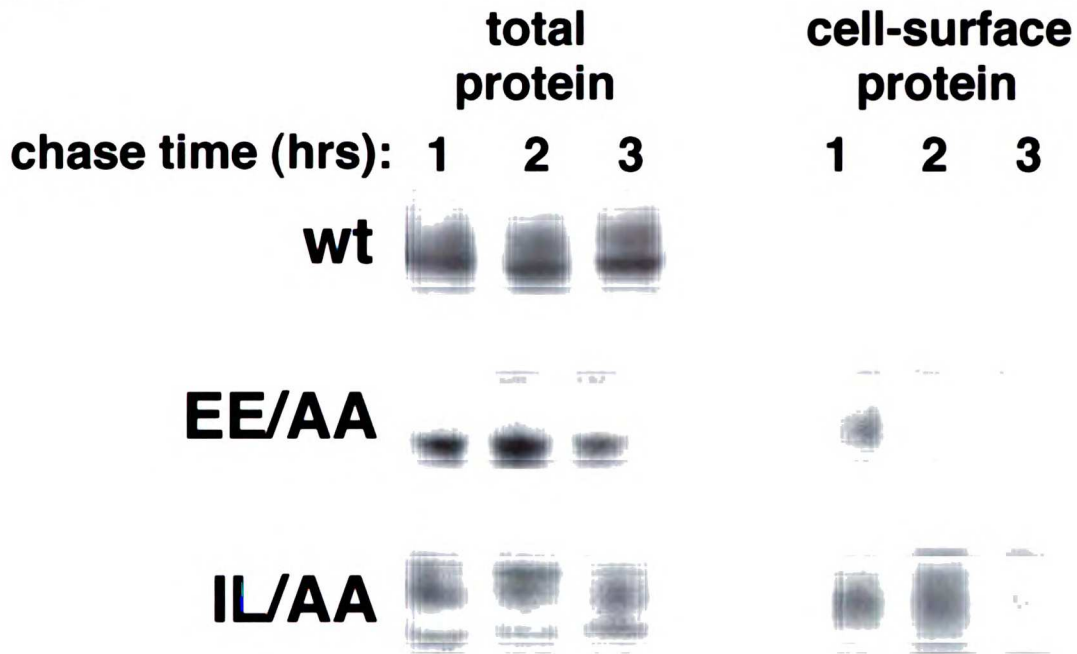


Figure 5. VMAT2 mutants IL/AA and EE/AA enter the constitutive secretory pathway

(A) Cells were labeled with 0.5 mCi/ml ³⁵S-cysteine/methionine for 30 minutes, then incubated for 1, 2, or 3 hours with unlabeled cysteine and methionine. To measure how much ³⁵S-labeled VMAT2 was delivered to the cell surface during each timepoint, HA.11 antibody was added to the medium of half the cells during their last hour of chase. The remaining cells were used to measure total ³⁵S-labeled VMAT2 at each timepoint. Total or cell-surface VMAT2 was then immunoprecipitated from solubilized cell extracts and submitted to autoradiography. Total protein (left panels) and cell-surface protein (right panels) are shown for wild-type, EE/AA, and IL/AA VMAT2 at each chase timepoint. Wild-type protein is virtually undetectable at the cell surface for all timepoints. In contrast, EE/AA and IL/AA begin to appear at the cell surface within an hour of synthesis and continue to appear there for at least 3 hours.

(B) For each VMAT2 construct (wt, EE/AA, and IL/AA), the pulse-chase analysis shown in (A) was performed three times. After autoradiography, films were optically scanned, digitized, and quantified using NIH Image. For each timepoint, cell-surface VMAT2 was expressed as a fraction of total VMAT2. Values from the three experiments were averaged and standard deviations calculated (error bars).

A



B

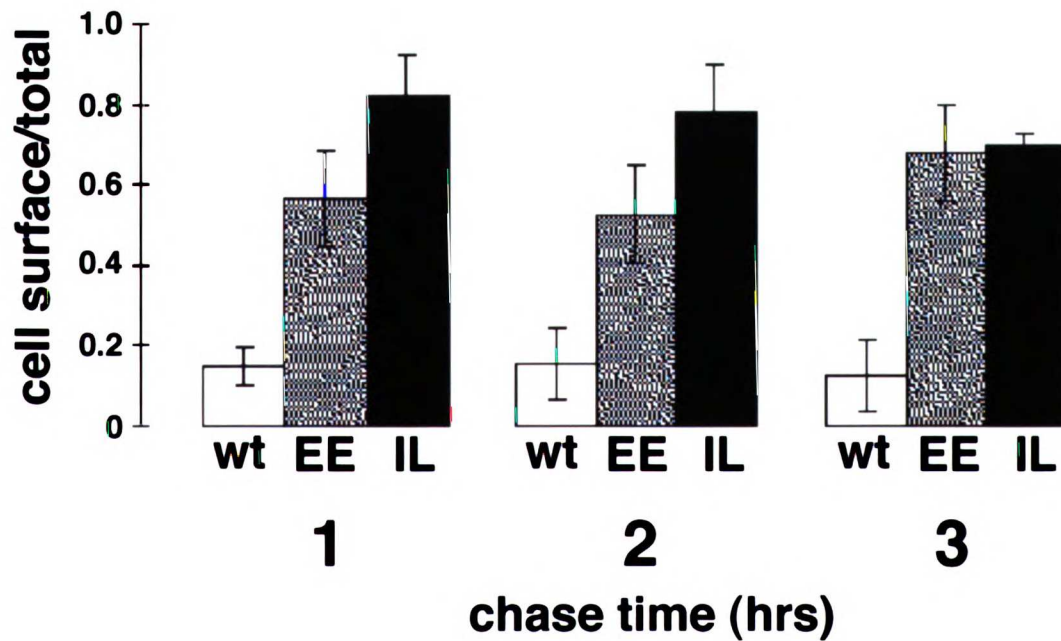
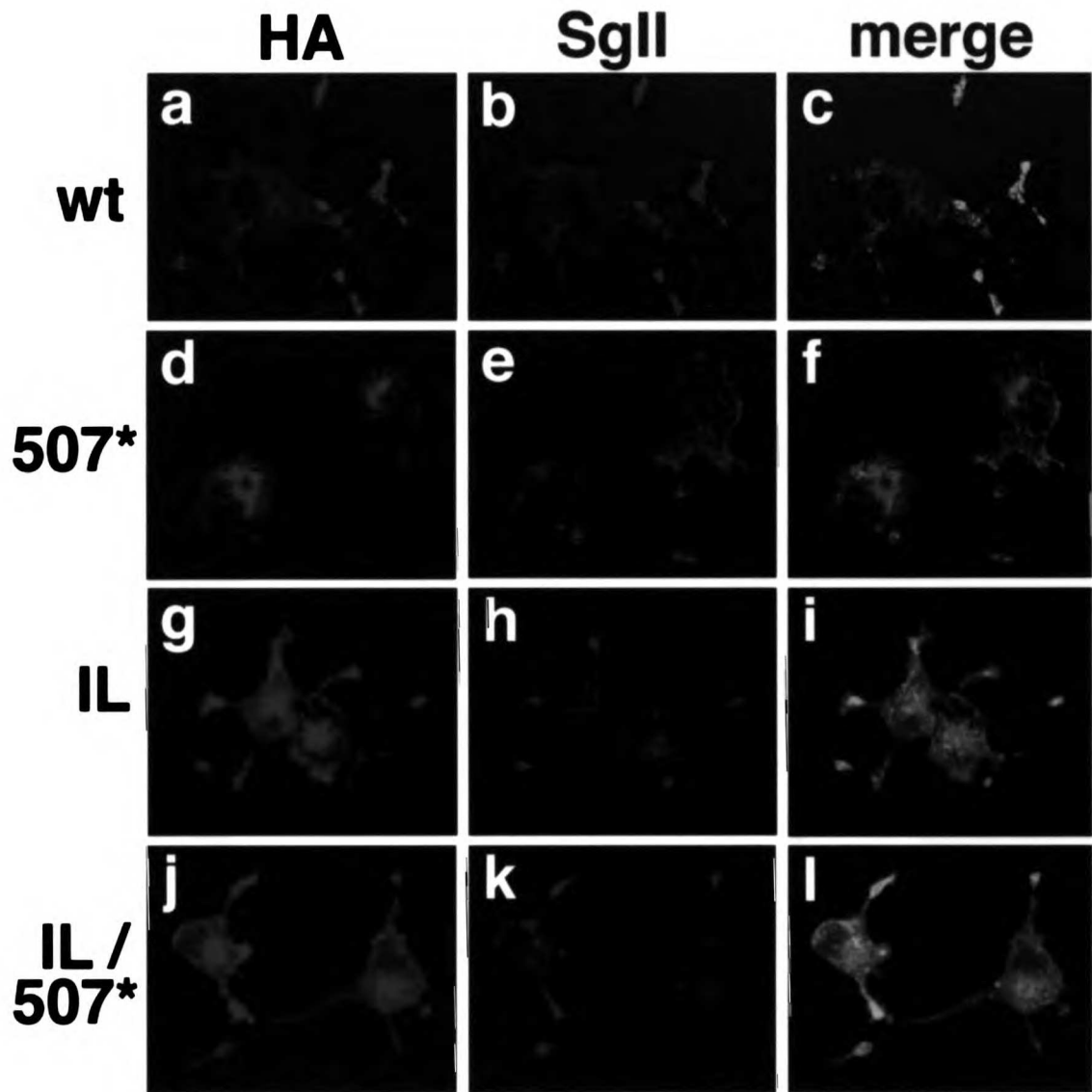


Figure 6. The IL motif acts prior to the acidic cluster motif in VMAT2 sorting

PC12 cells stably expressing wild-type VMAT2, the 507* deletion, the IL/AA mutation, and the IL/AA507* double mutation were double-stained with a mouse monoclonal antibody to the HA epitope (a, d, g, j) and a rabbit polyclonal antiserum to SgII (b, e, h, k). Secondary anti-mouse antibodies conjugated to Cy3 (a, d, g, j) or anti-rabbit antibodies conjugated to Cy5 (b, e, h, k) were used to visualize the proteins, and the cells were examined by confocal microscopy. The merged Cy3 and Cy5 images are shown in c, f, i, and l. Wild-type VMAT2 colocalizes with SgII, appearing primarily at the tips of processes (a-c). In contrast, neither 507* nor IL/AA colocalize with SgII. 507* appears almost exclusively in the perinuclear region (d-f), while IL/AA appears on the plasma membrane (g-i). The distribution of IL/AA507* looks identical to that of IL/AA (j-l), suggesting that the sorting step mediated by the IL motif occurs before the step mediated by the acidic cluster.



CHAPTER 4

Conclusions and Future Directions

Conclusions

Many studies have attempted to identify signals that target integral membrane proteins to regulated secretory vesicles. Although several targeting motifs have been identified, none is specific for sorting to LDCVs. By studying a protein that localizes almost exclusively to LDCVs, this thesis has been able to demonstrate the first examples of specific LDCV targeting and retention motifs. These studies are an important first step toward identifying the cytosolic machinery that underlies LDCV formation, and toward understanding the precise role of LDCV-mediated signaling in the brain.

We have identified the two motifs that are responsible for VMAT2 localization to LDCVs. The dileucine-like motif, particularly the two glutamates and the IL signal, appears necessary for targeting VMAT2 to newly-formed LDCVs in the TGN. Replacement of either the glutamates or the IL signal with alanine redirects VMAT2 from the regulated into the constitutive secretory pathway, resulting in its delivery to the plasma membrane. These mutations demonstrate the importance of the KEEKMAIL motif in targeting VMAT2 to LDCVs. The acidic cluster motif is required for the retention of VMAT2 on LDCVs during their maturation. Deletion of the acidic cluster or phosphorylation of the serines appears to promote the removal of VMAT2 from LDCVs. Thus, phosphorylation of the acidic cluster appears to inactivate its retention mechanism, and may provide cells with a way of regulating VMAT2 localization to LDCVs.

Future Directions

Identifying cytosolic proteins involved in LDCV targeting

Now that these targeting motifs have been identified, one important next step is to identify the cytosolic machinery responsible for sorting integral membrane proteins into LDCVs. Since the VMAT2 sorting motifs presumably interact with such machinery, we can look for proteins that bind to these motifs, either with the yeast two-hybrid system or with other protein binding assays. We have already shown that the phosphorylated acidic cluster motif in VMAT2 interacts with the cytoplasmic protein PACS-1, which mediates the removal of VMAT2 from LDCVs. However, since the unphosphorylated acidic cluster is required for VMAT2 retention on LDCVs, it is possible that a second, currently unidentified protein interacts with the unphosphorylated cluster to mediate retention. Such a protein could be identified by performing a yeast two hybrid screen using the VMAT2 AA mutant, which mimics the constitutively unphosphorylated state, as bait.

Dileucine motifs are known to interact with AP-1,2, and 3 complexes, and one of these complexes could interact with the KEEKMAIL sequence to mediate VMAT2 sorting into LDCVs. A directed yeast two hybrid screen or biochemical protein binding assay can be used to assess whether VMAT2 interacts with any of these adaptors, or with the newly-identified AP-4 complex. These types of experiments can also be used to look for novel adaptor complexes or other cytoplasmic proteins that might interact with dileucine-based motifs.

If interacting proteins are found, their functional involvement in VMAT2 trafficking and LDCV formation will need to be investigated. This can be done by functionally inactivating the protein(s) of interest in at least two ways. One way is to abolish expression of the protein by introducing antisense mRNA into PC12 cells. After determining that expression of the specified protein has been eliminated, effects on VMAT2 localization and LDCV formation in these cells can be examined. This approach was successfully used to study the role of PACS-1 in furin trafficking. When PACS-1 antisense mRNA was introduced into cells, furin trafficking was disrupted, confirming that PACS-1 is required for the proper localization of furin (Wan et al., 1998). However, antisense technology is unreliable. In addition to abolishing expression of the protein of interest, it can also disrupt the expression of other proteins and other cellular processes.

A second, more specific way of functionally inactivating a protein is to use a dominant-negative approach. This approach requires the protein(s) of interest to have multiple subunits or binding partners, and the VMAT2 binding site(s) to be well-characterized, but can potentially yield more interpretable results than the antisense RNA method. To use this approach, one would first identify and then mutate the VMAT2 binding site of a given protein, then overexpress the subunit containing this mutation in PC12 cells. The mutant subunit will bind to the other active subunits of the protein, creating a dominant-negative protein that is normal in most respects but incapable of

binding VMAT2. By expressing this subunit in cells stably expressing VMAT2, the effects of a given dominant-negative protein on VMAT2 localization and LDCV formation could be assessed. This approach has been successfully used to study the roles of several proteins involved in sorting, including clathrin, AP-2, and β -arrestin (Krupnick et al., 1997; Liu et al., 1998; Nesterov et al., 1999).

Investigating somatodendritic vs. axonal monoamine release

In addition to identifying the cytoplasmic proteins involved in LDCV targeting, a second important step is to use these targeting motifs to study monoamine release in the brain.

As discussed earlier, monoamines are released both somatodendritically and from nerve terminals, consistent with the localization of VMAT2 to both SVs and LDCVs in the brain. Although axonal release is thought to mediate rapid neurotransmission and somatodendritic release to modulate neuronal activity, the specific effects of each type of monoamine release on physiology and behavior are unknown. By introducing several of our VMAT2 mutants into VMAT2 knockout mice, it should be possible to selectively block or enhance monoamine release from particular populations of secretory vesicles. For instance, the 507* deletion of the acidic cluster motif or replacement of serines in the motif with aspartate (the DD mutant) both prevent VMAT2 localization to mature LDCVs, and thus monoamine uptake into these vesicles. If 507* or DD were expressed in a mouse, one could examine what effects the elimination of monoamine release from

mature LDCVs has on behavior and physiology. Conversely, replacement of acidic cluster serines with alanine (the AA mutant) promotes VMAT2 retention on LDCVs, and may result in increased localization to LDCVs. This mutant therefore could potentially be used to examine the effects of increased monoamine release from LDCVs. The EE/AA mutation appears to increase the localization of VMAT2 to synaptic vesicles and decrease its localization to LDCVs, and thus could be used to study what effects increased monoamine release from SVs has on physiology. Such studies could provide important insights into the roles of somatodendritic and axonal monoamine release on neuronal physiology, and help elucidate what role monoamines play in a variety of behaviors.

References

- Aghajanian, G. K., and Bunney, B. S. (1974). Pre- and postsynaptic feedback mechanisms in central dopaminergic neurons. In *Frontiers of Neurology and Neuroscience Research*, P. Seeman and G. M. Brown, eds. (Toronto: University of Toronto Press), pp. 4-11.
- Bauerfeind, R., and Huttner, W. B. (1993). Biogenesis of constitutive secretory vesicles, secretory granules and synaptic vesicles. *Curr. Opin. Cell Biol.* 5, 628-635.
- Bellocchio, E. E., Reimer, R. J., Fremeau, R. T., and Edwards, R. H. (2000). Uptake of glutamate into synaptic vesicles by an inorganic phosphate transporter. *Science* 289, 957-960.
- Blagoveshchenskaya, A. D., Hewitt, E. W., and Cutler, D. F. (1999). A complex web of signal-dependent trafficking underlies the triorganellar distribution of P-selectin in neuroendocrine PC12 cells. *J. Cell Biol.* 145, 1419-1433.
- Blagoveshchenskaya, A. D., Hewitt, E. W., and Cutler, D. F. (1999). Di-leucine signals mediate targeting of tyrosinase and synaptotagmin to synaptic-like microvesicles within PC12 cells. *Mol. Biol. Cell* 10, 3979-3990.
- Bruns, D., and Jahn, R. (1995). Real-time measurement of transmitter release from single synaptic vesicles. *Nature* 377, 62-65.
- Calakos, N., and Scheller, R. H. (1996). Synaptic vesicle biogenesis, docking, and fusion: a molecular description. *Physiol. Rev.* 76, 1-29.
- Cameron, P. L., Sudhof, T. C., Jahn, R., and de Camilli, P. (1991). Colocalization of synaptophysin with transferrin receptors: implications for synaptic vesicle biogenesis. *J. Cell Biol.* 115, 151-164.
- Chanat, E., and Huttner, W. B. (1991). Milieu-induced, selective aggregation of regulated secretory proteins in the trans-Golgi network. *J. Cell Biol.* 115, 1505-1519.
- Cheramy, A., Leviel, V., and Glowinski, J. (1981). Dendritic release of dopamine in the substantia nigra. *Nature* 289, 537-542.

Clift-O'Grady, L., Linstedt, A. D., Lowe, A. W., Grote, E., and Kelly, R. B. (1990). Biogenesis of synaptic vesicle-like structures in a pheochromocytoma cell line PC12. *J. Cell Biol.* *110*, 1693-1703.

De Camilli, P., and Jahn, R. (1990). Pathways to regulated exocytosis in neurons. *Ann. Rev. Physiol.* *52*, 625-645.

Dell'Angelica, E. C., Mullins, C., and Bonifacino, J. S. (1998). AP-4, a novel protein complex related to clathrin adaptors. *PNAS*.

Dietrich, J., Kastrup, J., Nielsen, B. L., Odum, N., and Geisler, C. (1997). Regulation and function of the CD3 gamma DXXXLL motif: A binding site for adaptor protein-1 and adaptor protein-2 in vitro. *J. Cell Biol.* *138*, 271-281.

Dittie, A. S., Hajibagheri, N., and Tooze, S. A. (1996). The AP-1 adaptor complex binds to immature secretory granules from PC12 cells, and is regulated by ADP-ribosylation factor. *J. of Cell Biol.* *132*, 523-536.

Dittie, A. S., Thomas, L., Thomas, G., and Tooze, S. A. (1997). Interaction of furin in immature secretory granules from neuroendocrine cells with the AP-1 adaptor complex is modulated by casein kinase II. *EMBO J.* *16*, 4859-4870.

Erickson, J. D., Eiden, L. E., and Hoffman, B. J. (1992). Expression cloning of a reserpine-sensitive vesicular monoamine transporter. *Proc. Natl. Acad. Sci. USA* *89*, 10993-10997.

Erickson, J. D., Varoqui, H., Schafer, M. D., Modi, W., Diebler, M. F., Weihe, E., Rand, J., Eiden, L. E., Bonner, T. I., and Usdin, T. B. (1994). Functional identification of a vesicular acetylcholine transporter and its expression from a "cholinergic" gene locus. *J. Biol. Chem.* *269*, 21929-21932.

Farquhar, M. G., Reid, J. J., and Daniell, L. W. (1978). Intracellular transport and packaging of prolactin: a quantitative electron microscope autoradiographic study of mammothrophs dissociated from rat pituitaries. *Endocrinology* *102*, 296-311.

Faundez, V., Horng, J.-T., and Kelly, R. B. (1998). A function for the AP3 coat complex in synaptic vesicle formation from endosomes. *Cell* *93*, 423-432.

Geffen, L. B., Jessel, T. M., Cuello, A. C., and Iverson, L. L. (1976). Release of dopamine from dendrites in rat substantia nigra. *Nature* 260, 258-260.

Glenn, D. E., and Burgoyne, R. D. (1996). Botulinum neurotoxin light chains inhibit both Ca(2+)-induced and GTP analogue-induced catecholamine release from permeabilised adrenal chromaffin cells. *FEBS Lett.* 386, 137-140.

Grace, A. A., and Bunney, B. S. (1995). Electrophysiological properties of midbrain dopamine neurons. In *Psychopharmacology: The Fourth Generation of Progress*, F. E. Bloom and D. J. Kupfer, eds. (New York: Raven Press), pp. 163-178.

Greene, L. A., and Rein, G. (1978). Release, storage and uptake of catecholamines by a clonal cell line of nerve growth factor (NGF) responsive pheochromocytoma cells. *Brain Research* 129, 247-263.

Greene, L. A., and Tischler, A. S. (1976). Establishment of a noradrenergic clonal line of rat adrenal pheochromocytoma cells which respond to nerve growth factor. *Proc. Natl. Acad. Sci. USA* 73, 2424-2428.

Grote, E., Hao, M. K., Bennett, M. K., and Kelly, R. B. (1995). A targeting signal in VAMP regulating transport to synaptic vesicles. *Cell* 81, 581-589.

Heeringa, M. J., and Abercrombie, E. D. (1995). Biochemistry of somatodendritic dopamine release in substantia nigra: an in vivo comparison with striatal dopamine release. *J. Neurochem.* 65, 192-200.

Heilker, R., Manning-Krieg, U., Zuber, J. F., and Spiess, M. (1996). In vitro binding of clathrin adaptors to sorting signals correlates with endocytosis and basolateral sorting. *EMBO J* 15, 2893-2899.

Honing, S., Sandoval, I. V., and von Figura, K. (1998). A di-leucine-based motif in the cytoplasmic tail of LIMP-II and tyrosinase mediates selective binding of AP3. *EMBO J* 17, 1304-1314.

Hunziker, W., and Fumey, C. (1994). A di-leucine motif mediates endocytosis and basolateral sorting of macrophage IgG Fc receptors in MDCK cells. *EMBO J.* 13, 2963-2967.

Jaffe, E. H., Marty, A., Schulte, A., and Chow, R. H. (1998). Extrasynaptic vesicular transmitter release from the somata of substantia nigra neurons in rat midbrain slices. *J. Neurosci.* *18*, 3548-3553.

Jones, B. G., Thomas, L., Molloy, S. S., Thulin, C. D., Fry, M. D., Walsh, K. A., and Thomas, G. (1995). Intracellular trafficking of furin is modulated by the phosphorylation state of a casein kinase II site in its cytoplasmic tail. *EMBO J.* *14*, 5869-5883.

Kantheti, P., et al. (1998). Mutation in AP3 delta in the mocha mouse links endosomal transport to storage deficiency in platelets, melanosomes, and synaptic vesicles. *Neuron* *21*, 111-122.

Kelly, R. B. (1991). Secretory granule and synaptic vesicle formation. *Curr. Opin. Cell Biol.* *3*, 654-660.

Kelly, R. B. (1993). Storage and release of neurotransmitters. *Cell/Neuron* *72/10*, 43-53.

Kelly, R. B., and Grote, E. (1993). Protein targeting in the neuron. *Ann. Rev. Neurosci.* *16*, 95-127.

Kirchhausen, T., Bonifacino, J. S., and Riezman, H. (1997). Linking cargo to vesicle formation-receptor tail interactions with coat proteins. *Curr. Opin. Cell Biol.* *9*, 488-495.

Klumperman, J., Kuliawat, R., Griffith, J. M., Geuze, H. J., and Arvan, P. (1998). Mannose-6-phosphate receptors are sorted from immature secretory granules via adaptor protein AP-1, clathrin and syntaxin 6-positive vesicles. *J. Cell Biol.* *141*, 359-371.

Krantz, D. E., Peter, D., Liu, Y., and Edwards, R. H. (1997). Phosphorylation of a vesicular monoamine transporter by casein kinase II. *J. Biol. Chem.* *272*, 6752-6759.

Krantz, D. E., Waites, C., Oorschot, V., Liu, Y., Wilson, R. I., Tan, P. K., Klumperman, J., and Edwards, R. H. (2000). A phosphorylation site regulates sorting of the vesicular acetylcholine transporter to dense core vesicles. *J. Cell Biol.* *149*, 379-395.

Krupnick, J., Santini, F., Gagnon, A., Keen, J., and Benovic, J. (1997). Modulation of the arrestin-clathrin interaction in cells. Characterization of beta-arrestin dominant-negative mutants. *J Biol Chem* *272*, 32507-12.

Kuliawat, R., Klumperman, J., Ludwig, T., and Arvan, P. (1997). Differential sorting of lysosomal enzymes out of the regulated secretory pathway in pancreatic beta-cells. *J. Cell Biol.* *137*, 595-608.

Kunkel, T. A., Bebenek, K., and McClary, J. (1991). Efficient Site-Directed Mutagenesis Using Uracil-Containing DNA. *Meth. Enzymol.* *204*, 125-139.

Liu, S., Marks, M., and Brodsky, F. (1998). A dominant-negative clathrin mutant differentially affects trafficking of molecules with distinct sorting motifs in the class II major histocompatibility complex (MHC) pathway. *J Cell Biol* *140*, 1023-37.

Liu, Y., and Edwards, R. H. (1997a). Differential localization of vesicular acetylcholine and monoamine transporters in PC12 cells but not CHO cells. *J. Cell. Biol.* *139*, 907-916.

Liu, Y., and Edwards, R. H. (1997b). The role of vesicular transport proteins in synaptic transmission and neural degeneration. *Annu. Rev. Neurosci.* *20*, 125-156.

Liu, Y., Peter, D., Roghani, A., Schuldiner, S., Prive, G. G., Eisenberg, D., Brecha, N., and Edwards, R. H. (1992). A cDNA that suppresses MPP⁺ toxicity encodes a vesicular amine transporter. *Cell* *70*, 539-551.

Liu, Y., Roghani, A., and Edwards, R. H. (1992a). Gene transfer of a reserpine-sensitive mechanism of resistance to MPP⁺. *Proc. Natl. Acad. Sci. USA* *89*, 9074-9078.

Liu, Y., Schweitzer, E. S., Nirenberg, M. J., Pickel, V. M., Evans, C. J., and Edwards, R. H. (1994). Preferential localization of a vesicular monoamine transporter to dense core vesicles in PC12 cells. *J. Cell Biol.* *127*, 1419-1433.

Martin, T. F. J. (1994). The molecular machinery for fast and slow neurosecretion. *Curr. Opin. Neurobiol.* *4*, 626-632.

McIntire, S. L., Reimer, R. J., Schuske, K., Edwards, R. H., and Jorgensen, E. M. (1997). Identification and characterization of the vesicular GABA transporter. *Nature* *389*, 870-876.

Milgram, S. L., Mains, R. E., and Eipper, B. A. (1996). Identification of routing determinants in the cytosolic domain of a secretory granule-associated integral membrane protein. *J. Biol. Chem.* *271*, 17526-17535.

Molloy, S. S., Anderson, E. D., Jean, F., and Thomas, G. (1999). Bi-cycling the furin pathway: from TGN localization to pathogen activation and embryogenesis. *Trends in Cell Biol.* 9, 28-35.

Molloy, S. S., Thomas, L., Kamibayashi, C., Mumby, M. C., and Thomas, G. (1998). Regulation of endosome sorting by a specific PP2A isoform. *J. Cell Biol.* 142, 1399-1411.

Nesterov, A., Carter, R., Sorkina, T., Gill, G., and Sorkin, A. (1999). Inhibition of the receptor-binding function of clathrin adaptor protein AP-2 by dominant-negative mutant mu2 subunit and its effects on endocytosis. *EMBO J* 18, 2489-99.

Nirenberg, M. J., Chan, J., Liu, Y., Edwards, R. H., and Pickel, V. M. (1996). Ultrastructural localization of the monoamine transporter-2 in midbrain dopaminergic neurons: potential sites for somatodendritic storage and release of dopamine. *J. Neurosci.* 16, 4135-4145.

Nirenberg, M. J., Chan, J., Liu, Y., Edwards, R. H., and Pickel, V. M. (1997). Vesicular monoamine transporter-2: immunogold localization in striatal axons and terminals. *Synapse* 26, 194-198.

Nirenberg, M. J., Liu, Y., Peter, D., Edwards, R. H., and Pickel, V. M. (1995). The vesicular monoamine transporter-2 is present in small synaptic vesicles and preferentially localizes to large dense core vesicles in rat solitary tract nuclei. *Proc. Natl. Acad. Sci. USA* 92, 8773-8777.

Odorizzi, G., Cowles, C. R., and Emr, S. D. (1998). The AP3 complex: a coat of many colors. *Trends Cell Biol* 8, 282-288.

Ooi, C. E., Moreira, J. E., Dell'Angelica, E. C., Poy, G., Wassarman, D. A., and Bonifacino, J. S. (1997). Altered expression of a novel adaptin leads to defective pigment granule biogenesis in the *Drosophila* eye color mutant garnet. *EMBO J* 16, 4508-4518.

Orci, L., Ravazzola, M., Amherdt, M., Perrelet, A., Powell, S. K., Quinn, D. L., and Moore, H. P. (1987). The trans-most cisternae of the Golgi complex: a compartment for sorting of secretory and plasma membrane proteins. *Cell* 51, 1039-1051.

- Peter, D., Liu, Y., Sternini, C., de Giorgio, R., Brecha, N., and Edwards, R. H. (1995). Differential expression of two vesicular monoamine transporters. *J. Neurosci.* *15*, 6179-6188.
- Pond, L., Kuhn, L. A., Teyton, L., Schutze, M.-P., Tainer, J. A., Jackson, M. R., and Peterson, P. A. (1995). A role for acidic residues in di-leucine motif-based targeting to the endocytic pathway. *J. Biol. Chem.* *270*, 19989-19997.
- Rapoport, I., Chen, Y. C., Cupers, P., Shoelson, S. E., and Kirchhausen, T. (1998). Dileucine-based sorting signals bind to the beta chain of AP-1 at a site distinct and regulated differently from the tyrosine-based motif-binding site. *EMBO J.* *17*, 2148-2155.
- Regnier-Vigouroux, A., Tooze, S. A., and Huttner, W. B. (1991). Newly synthesized synaptophysin is transported to synaptic-like microvesicles via constitutive secretory vesicles and the plasma membrane. *EMBO J.* *10*, 3589-3601.
- Rindler, M. J. (1998). Carboxypeptidase E, a peripheral membrane protein implicated in the targeting of hormones to secretory granules, co-aggregates with granule content proteins at acidic pH. *J. Biol. Chem.* *273*, 31180-5.
- Robertson, G. S., Damsma, G., and Fibiger, H. C. (1991). Characterization of dopamine release in the substantia nigra by in vivo microdialysis in freely moving rats. *J. Neurosci.* *11*, 2209-2216.
- Roghani, A., Feldman, J., Kohan, S. A., Shirzadi, A., Gundersen, C. B., Brecha, N., and Edwards, R. H. (1994). Molecular cloning of a putative vesicular transporter for acetylcholine. *Proc. Natl. Acad. Sci. USA* *91*, 10620-10624.
- Sandoval, I. V., and Bakke, O. (1994). Targeting of membrane proteins to endosomes and lysosomes. *Trends Cell Biol* *4*, 292-297.
- Schafer, W., Stroh, A., Berghofer, S., Seiler, J., Vey, M., Kruse, M. L., Kern, H. F., Klenk, H. D., and W., G. (1995). Two independent targeting signals in the cytoplasmic domain determine trans-Golgi network localization and endosomal trafficking of the proprotein convertase furin. *EMBO J.* *4*, 2424-2435.
- Schmidle, T., Weiler, R., Desnos, C., Scherman, D., Fischer-Colbrie, R., Floor, E., and H., W. (1991). Synaptin/synaptophysin, p65 and SV2: their presence in adrenal

chromaffin granules and sympathetic large dense core vesicles. *Biochim. Biophys. Acta.* 1060, 251-256.

Simpson, F., Peden, A. A., Christopolou, L., and Robinson, M. S. (1997). Characterization of the adaptor-related protein complex, AP3. *J. Cell Biol.* 137, 835-845.

Sudhof, T. C. (1995). The synaptic vesicle cycle: a cascade of protein-protein interactions. *Nature* 375, 645-653.

Tan, P. K., Waites, C., Liu, Y., Krantz, D. E., and Edwards, R. H. (1998). A leucine-based motif mediates the endocytosis of vesicular monoamine and acetylcholine transporters. *J. Biol. Chem.* 273, 17351-17360.

Tooze, J., and Tooze, S. A. (1986). Clathrin-coated vesicular transport of secretory proteins during the formation of ACTH-containing secretory granules in AtT20 cells. *J. Cell Biol.* 103, 839-850.

Tooze, S. A., Chanut, E., Tooze, J., and Huttner, W. B. (1993). Secretory granule formation. In *Mechanisms of intracellular trafficking and processing of proproteins*: CRC Press), pp. 157-177.

Tooze, S. A., Flatmark, T., Tooze, J., and Huttner, W. B. (1991). Characterization of the immature secretory granule, an intermediate in granule biogenesis. *J. Cell Biol.* 115, 1491-1503.

Tooze, S. A., and Huttner, W. B. (1990). Cell-free protein sorting to the regulated and constitutive secretory pathways. *Cell* 60, 837-847.

Varoqui, H., and Erickson, J. D. (1998). The cytoplasmic tail of the vesicular acetylcholine transporter contains a synaptic vesicle targeting signal. *J. Biol. Chem.* 273, 9094-9098.

Varoqui, H., and Erickson, J. D. (1997). Vesicular neurotransmitter transporters. Potential sites for the regulation of synaptic function. *Molec. Neurobiol.* 15, 165-191.

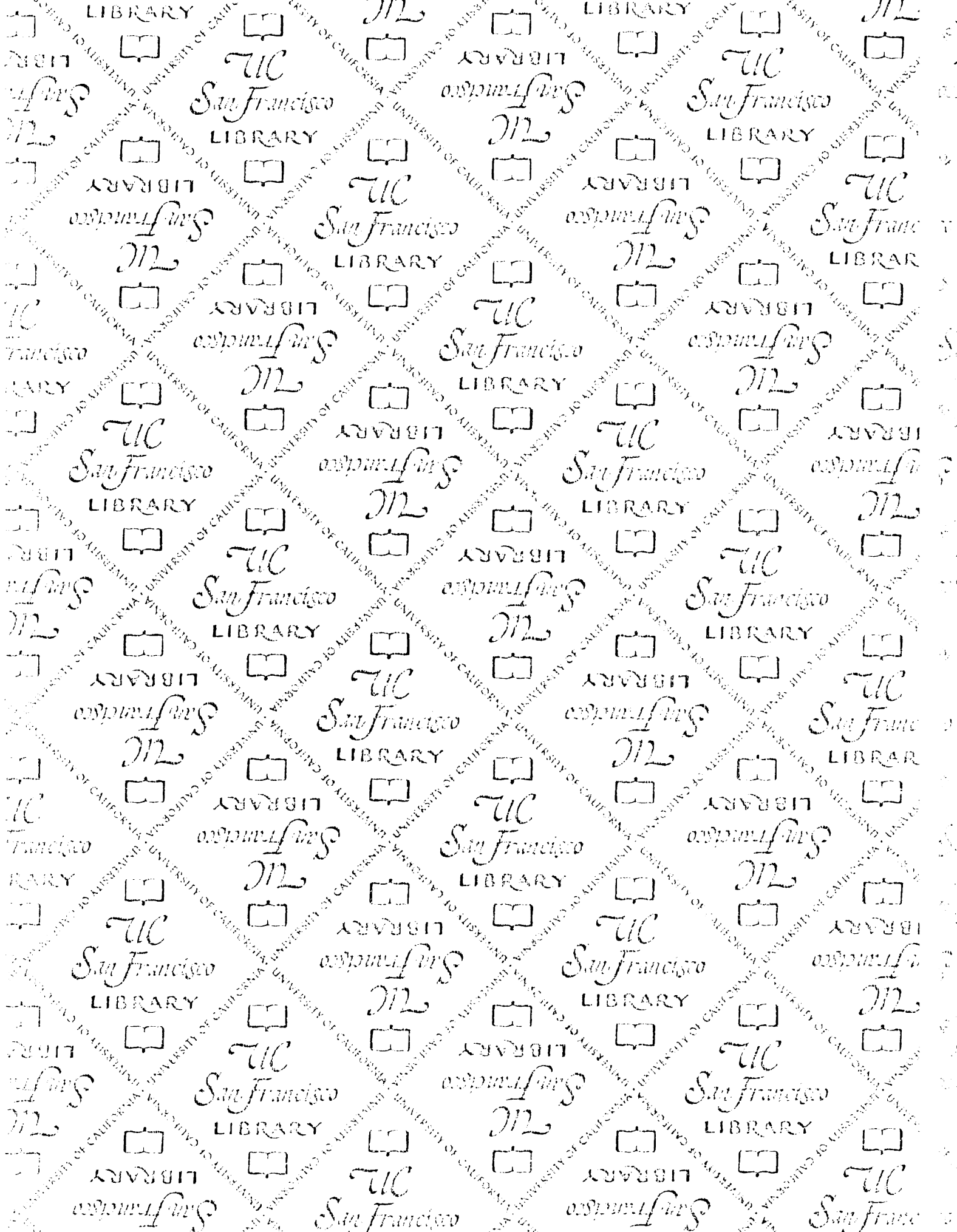
Waites, C. L., Mehta, A., Tan, P. K., Thomas, G., Edwards, R. H., and Krantz, D. E. (2001). An acidic motif retains vesicular monoamine transporter 2 on large dense core vesicles. *J. Cell Biol.* 152, 1159-1168.

Walch-Solimena, C., Takei, K., Marek, K. L., Midyett, K., Sudhof, T. C., De Camilli, P., and Jahn, R. (1993). Synaptotagmin: a membrane constituent of neuropeptide-containing large dense-core vesicles. *J. Neurosci.* *13*, 3895-3903.

Wan, L., Molloy, S. S., Thomas, L., Liu, G., Xiang, Y., Rybak, S. L., and Thomas, G. (1998). PACS-1 defines a novel gene family of cytosolic sorting proteins required for trans-Golgi network localization. *Cell* *94*, 205-216.

Weihe, E., Schafer, M. K., Erickson, J. D., and Eiden, L. E. (1994). Localization of vesicular monoamine transporter isoforms (VMAT1 and VMAT2) to endocrine cells and neurons in rat. *J. Mol. Neurosci.* *5*, 149-164.

Xiang, Y., Molloy, S. S., Thomas, L., and Thomas, G. (2000). The PC6B cytoplasmic domain contains two acidic clusters that direct sorting to distinct trans-Golgi network/endosomal compartments. *Mol. Biol. Cell* *11*, 1257-1273.



For reference

Not to be taken from the room.

7065744



3 1378 00706 5744

